NIST-GCR-95-685

CHEMICAL INHIBITION OF METHANE-AIR DIFFUSION FLAME

K. Seshadri

Center for Energy and Combustion Research
Department of Applied Mechanics and Engineering Sciences
University of California at San Diego
La Jolla, CA 92093-0411

Issued June 1996

U.S. Department of Commerce
Michael Kantor, *Secretary*
Technology Administration
Mary L. Good, *Under Secretary for Technology*
National Institute of Standards and Technology
Arati Prabhakar, *Director*

Notice

This report was prepared for the Building and Fire Research Laboratory of the National Institute of Standards and Technology under grant number 60NANB3D1435. The statement and conclusions contained in this report are those of the authors and do not necessarily reflect the views of the National Institute of Standards and Technology or the Building and Fire Research Laboratory.

FINAL REPORT
Chemical Inhibition of Methane-Air Diffusion Flame
Grant # NIST 60NANB3D1435

K. Seshadri

Center for Energy and Combustion Research
Department of Applied Mechanics and Engineering Sciences
University of California at San Diego
La Jolla, California 92093-0411

Abstract

The principal objective of this research is to clarify the mechanisms of chemical inhibition of methane-air diffusion flames by CF_3Br and CF_3H. An experimental, numerical and analytical study is conducted. In inhibited flames at conditions close to flame extinction significant amount of oxygen is found to leak through the reaction zone. Therefore an asymptotic analysis is performed to characterize the structure and critical conditions of extinction of uninhibited methane-air diffusion flames. Later this analyses is extended to methane-air diffusion flames inhibited with CF_3Br. Critical conditions of extinction of the flame are measured over a wide range with agents added to the air stream and to the fuel stream. Numerical calculations with detailed chemistry are performed to calculate the structure and critical conditions of flame extinction. The numerical results are compared with the measurements.

Introduction

The principal objective of this research is to obtain an improved understanding of the mechanisms of chemical inhibition of methane-air diffusion flames by CF_3Br. This research is conducted in collaboration with Professor N. Peters at the Institut für Technische Mechanik, RWTH Aachen, Germany. The results of this research are summarized in the publications and reports listed below

1. K. Seshadri and N. Ilincic, "The Asymptotic Structure of Nonpremixed Methane-Air Flames with Oxidizer Leakage of Order Unity," Combustion and Flame **101**: 69–80 (1995).

2. K. Seshadri and N. Ilincic, "The Asymptotic Structure of Inhibited Nonpremixed Methane-Air Flames," Combustion and Flame **101**: 271–294 (1995).

3. D. Trees, A. Grudno, N. Ilincic, T. Weißweiler, and K. Seshadri, "Experimental and Numerical Studies on Chemical Inhibition of Methane-Air Diffusion Flames by CF_3Br and CF_3H," paper

presented at the Joint Technical Meeting, Central and Western States and Mexican National Section of the International Combustion Institute, San Antonio, Texas April 23–26 (1995).

These publications and reports are identified as Chapters 1, 2, and 3 in this report. These chapters also give in detail the motivation, the experimental and analytical approach and the conclusions of this study.

CHAPTER 1

The Asymptotic Structure of Nonpremixed Methane–Air Flames with Oxidizer Leakage of Order Unity

K. SESHADRI* and N. ILINCIC

Center for Energy and Combustion Science, Department of Applied Mechanics and Engineering Sciences, University of California at San Diego, La Jolla, CA 92093-0310

The asymptotic structure of nonpremixed methane–air flames is analyzed using a reduced three-step mechanism. The three global steps of this reduced mechanism are similar to those used in a previous analysis. The rates of the three steps are related to the rates of the elementary reactions appearing in the C_1-mechanism for oxidation of methane. The present asymptotic analysis differs from the previous analysis in that oxygen is presumed to leak from the reaction zone to the leading order. Chemical reactions are presumed to occur in three asymptotically thin layers: the fuel-consumption layer, the nonequilibrium layer for the water-gas shift reaction and the oxidation layer. The structure of the fuel-consumption layer is presumed to be identical to that analyzed previously and in this layer the fuel reacts with the radicals to form primarily CO and H_2 and some CO_2 and H_2O. In the oxidation layer the CO and H_2 formed in the fuel-consumption layer are oxidized to CO_2 and H_2O. The present analysis of the oxidation layer is simpler than the previous analysis because the variation in the values of the concentration of oxygen can be neglected to the leading order and this is a better representation of the flame structure in the vicinity of the critical conditions of extinction. The predictions of the critical conditions of extinction of the present model are compared with the predictions of previous models. It is anticipated that the present simple model can be easily extended to more complex problems such as pollutant formation in flames or chemical inhibition of flames.

INTRODUCTION

Rate-ratio asymptotic analyses using reduced three-step and four-step chemical–kinetic mechanisms have been successfully used previously to determine the structure and critical conditions of extinction of nonpremixed methane–air flames [1–6]. In these analyses it is assumed that fuel is completely consumed in the reaction zone and the oxygen leakage through the reaction zone is of order ϵ, where ϵ is the characteristic thickness of an asymptotically thin reaction layer in which a major fraction of the products are formed. For undiluted methane–air flames at conditions close to flame extinction, the results of Seshadri and Peters [1] and Yang and Seshadri [2] predict that roughly 30% of the oxygen in the original reactant stream leaks through the flame and the results of Chelliah and Williams [4] predict roughly 20% of the oxygen in the original reactant stream to leak through the flame. Therefore it appears that a better approximation of the flame structure in the vicinity of the critical conditions of flame extinction would be to assume that the oxygen leakage through the reaction zone is of order unity rather than of order ϵ. This assumption is also consistent with experimental measurements [7, 8] of the flame structure which show significant leakage of oxygen through the reaction zone at conditions close to extinction. In view of these observations an alternative and simpler analysis of the flame structure is performed here with complete consumption of fuel in the reaction zone and with oxygen leakage from the reaction zone to the leading order. The results obtained from this simple model are compared with the results of the previous models [1, 2].

In a classical activation-energy asymptotic analysis of the structure of nonpremixed flames using one-step chemistry, Linan [9] identified four different combustion regimes: (i) an ignition regime at high values of the strain rates, where there is extensive interpenetration of fuel and oxygen through diffusion with the reaction widely distributed over the flow field, (ii) an unstable partial-burning regime at lower values of the strain rates, where there is a thin

* Corresponding author.

COMBUSTION AND FLAME 101: 69–80 (1995)

Published by Elsevier Science Inc.

0010-2180/95/$9.50
SSDI 0010-2180(94)00172-O

reaction zone with leakage of fuel and oxygen through the reaction zone to the leading order, (iii) a premixed-flame regime, where there is a thin reaction zone with leakage of one of the reactants through the reaction zone to the leading order depending on the stoichiometry of the overall reaction and the ambient temperature of the reactants, thereby causing the structure of the reaction zone in this regime to resemble that of a nonadiabatic premixed flame, and (iv) a diffusion-flame regime at the lowest values of the strain rates, where there is a thin reaction zone through which neither reactant leaks to the leading order, causing the profiles outside the reaction zone to be the chemical-equilibrium profiles of the Burke-Schumann limit [10]. The critical strain rate at ignition was deduced by Linan [9] by analyzing the structure of the diffusion flame in the ignition regime and the critical strain rate at extinction was deduced by analyzing the structure of the diffusion flame in the premixed-flame regime and the diffusion-flame regime. The structure of a steady diffusion flame at low rates of strain can be expected to be represented by the diffusion-flame regime. As the strain rate is increased leakage of the reactants through the flame increases and the structure of the flame can be expected to be represented by the premixed-flame regime at conditions close to flame extinction. For most hydrocarbon-air flames, the overall stoichiometry of the one-step chemical reaction between the fuel and oxygen is such that the activation-energy analysis of Linan [9] of the premixed-flame regime predicts fuel leakage through the reaction zone to the leading order, because only in this case it is possible to match the inner structure with the outer structure of the flame. This is one of the principal deficiencies of activation-energy asymptotic models because measurements show oxygen leakage and not fuel leakage from the reaction zone [7, 8].

The asymptotic analysis performed here employs techniques developed by Seshadri and Peters [1] for analyzing the structure of methane-air diffusion flames using a reduced three-step mechanism. In this previous analysis [1] the outer structure was presumed to be similar to the outer structure of the flame in the diffusion-flame regime analyzed by Linan [9] with complete consumption of fuel and oxygen in the reaction zone to the leading order. In the analysis developed here the outer structure is presumed to be similar to the outer structure of the flame in the premixed-flame regime analyzed by Linan [9]. However, oxygen rather than fuel is presumed to leak from the reaction zone to the leading order. Matching between the outer and the inner structures is still possible because multiple-step chemistry is employed in the analysis and the activation-energies of the elementary reactions contributing to the rate of the overall reactions in the reduced chemical-kinetic mechanism are not presumed to be large. Thus one of the principal deficiencies of activation-energy asymptotic analysis is rectified by use of multiple-step chemistry. The intent of the present analysis is primarily to illustrate the technique for analyzing the flame structure with oxygen leakage through the reaction zone to the leading order. Therefore only the rates of the principal elementary reactions contributing to the rates of the overall reactions in the reduced mechanism are considered here. For improved numerical accuracy the influence of additional reactions can be readily included using the techniques developed by Yang and Seshadri [2].

REDUCED CHEMICAL-KINETIC MECHANISM

Peters and Rogg [11] have outlined a detailed chemical-kinetic mechanism for describing the oxidation of a number of hydrocarbon fuels including that of methane. This mechanism was used to predict the structure and critical conditions of extinction of nonpremixed methane-air flames over a wide parametric range [12] and the results were found to agree fairly well with measurements. Calculations were also performed with a five-step and a four-step reduced mechanism deduced from this detailed mechanism and the results were found to agree well with those calculated using the detailed mechanism [12]. Therefore the rate data used here are identical to those shown in Table 1.1 of Ref. 11.

Peters [13] has outlined a systematic procedure for deducing reduced chemical-kinetic mechanisms from detailed mechanisms. For methane-air flames the principal path of oxidation is found to be $CH_4 \rightarrow CH_3 \rightarrow CH_2O \rightarrow HCO \rightarrow CO$, $H_2 \rightarrow CO_2$, H_2O [12]. The radicals H, OH, O, the unstable species HO_2 and the stable species O_2 participate in chemical reactions along this principal path. If steady-state approximations are introduced for the species CH_3, CH_2O, HCO, OH, H, O, and HO_2 [1, 13], the three-step mechanism

$$CH_4 + O_2 \rightarrow CO + H_2 + H_2O, \quad \text{I}$$

$$CO + H_2O = CO_2 + H_2, \quad \text{II}$$

$$O_2 + 2H_2 \rightarrow 2H_2O, \quad \text{III}$$

is obtained. This three-step mechanism is identical to that used previously [1]. For simplicity the overall reactions I and III are presumed to be irreversible [1]. The overall reaction I is effectively a chain-breaking step and represents the reaction between CH_4 and the radicals to form the intermediate products CO and H_2. The overall reaction II represents the oxidation of CO to form the final product CO_2 and the overall reaction III represents the radical recombination steps and is also responsible for a major fraction of the heat released in the flame. The principal elementary reactions contributing to the rates of the overall reactions I, II, and III are [1, 2, 12]

$$11.\ CH_4 + H \rightarrow CH_3 + H_2,$$

$$10.\ CO + OH = CO_2 + H,$$

$$5.\ H + O_2 + M \rightarrow HO_2 + M,$$

respectively, where M represents any third body and the elementary reactions are identified using the same numbers as those shown in Table 1 of Ref. 1 so that the results can be easily compared with those obtained previously [1]. The rate of the overall reaction I is the forward rate of the elementary step 11 and the rate constant for this reaction is $k_{11} = 2.2 \times 10^4 T^{3.0} \exp(-4402/T)$, where T is the temperature. The forward and backward rates of the overall reaction II are the forward and backward rates of the elementary reaction 10 and rate constants for these reactions are $k_{10f} = 4.40 \times 10^6 T^{1.5} \exp(373/T)$ and $k_{10b} = 4.956 \times 10^8 T^{1.5} \exp(-10796/T)$, where subscripts f and b refer respectively to the forward and backward steps of any reaction. The rate of the overall reaction III is the forward rate of the elementary step 5 and the rate constant for this reaction is $k_5 = 2.3 \times 10^{18} T^{-0.8}$. The concentration of the third body is calculated using the relation $C_M = [p\overline{W}/(\hat{R}T)] \sum_{i=1}^{N} \eta_i Y_i / W_i$ where subscript i denotes the species i, p denotes the pressure, $\overline{W}$ the average molecular weight, $\hat{R}$ the gas constant, Y_i, W_i, and η_i are respectively the mass fraction, the molecular weight and the Chaperon efficiency of species i. For simplicity, only the mass fractions of H_2O, CO_2, and N_2 are used to calculate the value of C_M and their values are presumed to be equal to that for stoichiometric combustion of methane and air by a one-step reaction to form H_2O and CO_2. The values of η_i used in the calculations are 6.5, 1.5, and 0.4, respectively, for H_2O, CO_2, and N_2.

The overall reaction rates for the reduced mechanism contain the concentration of the hydroxyl radical C_{OH}. The value of C_{OH} is calculated assuming that the elementary reaction

$$3.\ OH + H_2 = H_2O + H$$

is in partial equilibrium [1, 2, 12]. Thus $C_{OH} = C_H C_{H_2O} / (K_3 C_{H_2})$, where $K_3 = 0.232 \exp(7537/T)$ is the equilibrium constant of the elementary step 3. To express the rates of the overall reactions in terms of the species appearing in the three-step mechanism, it is necessary to obtain an explicit algebraic expression for C_H. The steady-state concentration of the radical H can be obtained by equating the net rate of the reversible chain-branching step

$$1.\ H + O_2 = OH + O$$

to the sum of the rates of chain-breaking steps 11 and 5. The rate of the elementary step 1 contains the concentration of the radical O, which is calculated assuming that the re-

versible elementary reaction

$$2.\ H_2 + O = OH + H$$

is in partial equilibrium [1]. Thus $C_O = C_{H_2O}C_H{}^2/(K_2K_3C_{H_2}{}^2)$, where $K_2 = 2.277\exp(-963/T)$ is the equilibrium constant of the elementary step 2. The steady-state concentration of the radical H can now be written as [1]

$$C_H = \frac{K_1{}^{1/2}K_2{}^{1/2}K_3C_{H_2}{}^{3/2}C_{O_2}{}^{1/2}}{C_{H_2O}} \times\left(1 - \frac{k_{11}C_F}{k_{1f}C_{O_2}} - \frac{k_5C_M}{k_{1f}}\right)^{1/2}, \qquad (1)$$

where subscript F refers to the fuel, $k_{1f} = 2.0 \times 10^{14}\exp(-8456/T)$ and $K_1 = 12.76\exp(-8032/T)$ are the forward rate constant and the equilibrium constant of the elementary chain-branching step 1.

THE BASIC STRUCTURE

Figures 1a and 1b show a schematic illustration of the basic flame structure. Figure 1a shows the overall outer structure with the infinitely thin flame located at $Z = Z_p$, where Z represents the mixture fraction and its definition is similar to that employed by Peters [14] and the subscript p denotes condtions at the infinitely thin reaction zone. The ambient oxidizer stream is at $Z = 0$ and the ambient fuel stream at $Z = 1$. The outer structure is similar to the outer structure of the nonpremixed flame in the premixed-flame regime of Linan [9] with leakage of oxygen through the reaction zone to the leading order. The maximum flame temperature T_p in the limit of infinitely fast chemical reactions is less than the adiabatic flame temperature T_{st} calculated in the chemical-equilibrium Burke–Schumann limit [9, 10]. In the outer structure of the flame, the region $Z > Z_p$ represents frozen flow and the region $Z < Z_p$ represents equilibrium flow with $Y_F = 0$ in the leading order.

The inner structure of the flame is presumed to be identical to that analyzed in Ref. 1 and consists of a thin fuel-consumption layer of thickness of order δ and a thin oxidation layer of thickness of order ϵ. The water-gas shift reaction II is presumed to be in equilibrium everywhere except in a thin layer of thickness of order ν. The ordering $\delta < \nu \ll \epsilon \ll 1$ is used in the analysis. The relative location of these layers with respect to each other in terms of η is shown in Fig. 1b, where η represents a stretched independent variable used in the analysis of the oxidation layer. Due to finite rates of the overall reactions the maximum flame temperature T^0 is less than T_p and it is the characteristic temperature at the fuel-consumption layer. The fuel-consumption layer is presumed to be located at $Z = Z_p$ and in this layer the fuel reacts with the radicals in accordance with the overall reaction I to primarily form CO and H_2 and some CO_2 and H_2O. Oxygen leaks through the fuel-consumption layer to the leading order. In the oxidation layer the concentration of the fuel is presumed to be zero and in this layer CO and H_2 are oxidized to form H_2O and CO_2. In the region $Z > Z_p$ the concentration of radicals is zero, therefore this region is chemically inert.

THE OUTER STRUCTURE

The outer structure of the flame is presumed to be governed by the overall one-step reaction $CH_4 + 2O_2 \rightarrow CO_2 + 2H_2O$ and the Lewis numbers $L_i = \lambda/(\rho c_p D_i)$ of the species appearing in the one-step reaction are presumed to differ from unity by a quantity of order ϵ. Here λ, ρ, and c_p denote the coefficient of thermal conductivity, the density and the heat capacity of the gas mixture and D_i is the coefficient of diffusion of species i. If the heat capacity is presumed to be a constant, then the coupling relations between the temperature and the mass fractions of CH_4, O_2, H_2O, and CO_2 can be written as

$$Y_F/W_F = Y_{F,1}Z/W_F - (T - T_u(Z))c_p/(-\Delta H),$$

$$Y_{O_2}/(2W_{O_2}) = Y_{O_2,2}(1 - Z)/(2W_{O_2}) - (T - T_u(Z))c_p/(-\Delta H),$$

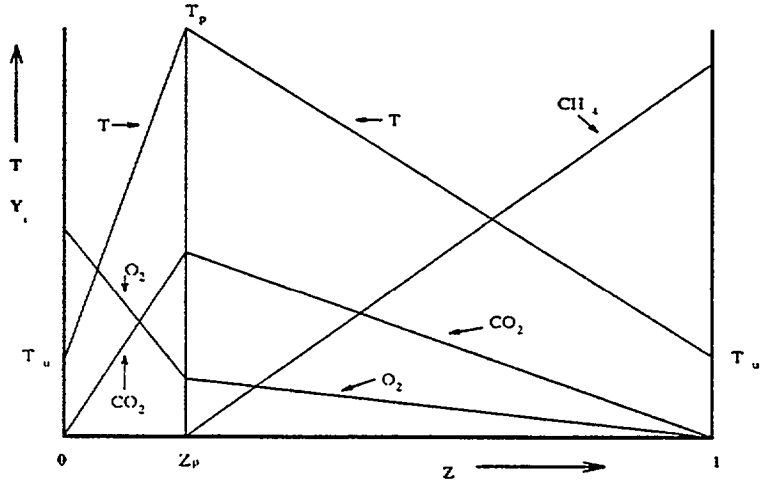

(a)

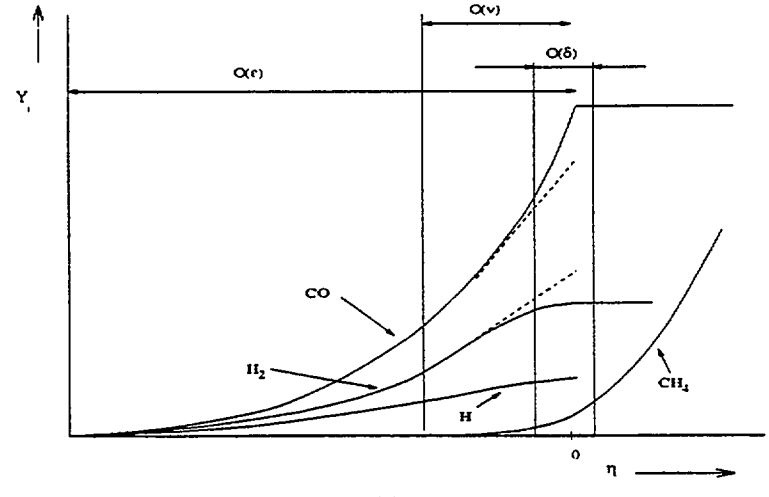

(b)

Fig. 1. (a). Schematic illustration of the outer structure. (b). Schematic illustration of the inner structure showing the fuel-consumption layer, the layer where the global reaction II is not in equilibrium, and the oxidation layer.

$$Y_{H_2O}/(2W_{H_2O}) = Y_{CO_2}/W_{CO_2} = (T - T_u(Z))c_p/(-\Delta H), \quad (2)$$

where $(-\Delta H)$ denotes the heat release in the one-step reaction, $T_u(Z) = T_2 + (T_1 - T_2)Z$ and the subscripts 1 and 2 refer to conditions at the ambient fuel stream and the ambient oxidizer stream respectively. In the Burke–Schumann limit, which corresponds to the diffusion-flame limit of Linan [9], the adiabatic flame temperature T_{st} and the flame position Z_{st} determined by setting $Y_F = Y_{O_2} = 0$ in Eq. 2 are

$$Z_{st} = \left[1 + 2Y_{F,1}W_{O_2}/(Y_{O_2,2}W_F)\right]^{-1},$$

$$T_{st} = T_u(Z_{st}) + Y_{F,1}Z_{st}(-\Delta H)/(c_pW_F). \quad (3)$$

At the position of the thin flame Z_p, the mass fraction of the fuel $Y_F = 0$. Thus it follows from Eqs. 2 and 3 that

$$T_p = T_u(Z_p) + (T_{st} - T_u(Z_{st}))Z_p/Z_{st},$$

$$Y_{O_2,p} = Y_{O_2,2}(1 - Z_p/Z_{st}),$$

$$Y_{H_2O,p}/(2W_{H_2O}) = Y_{CO_2,p}/W_{CO_2} = Y_{F,1}Z_p/W_F, \quad (4)$$

where the quantity $Y_{O_2,p}$ represents the leakage of oxygen through the reaction zone to the leading order. For simplicity the definitions [1, 2]

$$X_i \equiv Y_i W_{N_2}/W_i, \qquad \tau \equiv (T - T_u(Z))/\phi_T,$$
$$\phi_T \equiv (T_{st} - T_u(Z_{st}))W_F/(Y_{F,1}Z_{st}W_{N_2}), \qquad (5)$$

are introduced. With $a \equiv Y_{F,1}W_{N_2}/W_F$ and $b \equiv Y_{O_2,2}W_{N_2}/(2W_{O_2}Z_{st})$, the coupling relations shown in Eqs. 2 can be written as

$$X_F + \tau = aZ, \qquad X_{O_2} + 2\tau = 2bZ_{st}(1 - Z),$$
$$X_{H_2O}/2 = X_{CO_2} = \tau. \qquad (6)$$

In the region $Z < Z_p$, there is equilibrium flow with $X_F = 0$. Hence from Eq. 6 the relations

$$d\tau/dZ = a,$$
$$dX_{O_2}/dZ = -2b, \qquad \text{for } Z < Z_p \qquad (7)$$

are obtained. In the region $Z > Z_p$ there is frozen flow and the profiles of τ and X_F are linear functions of Z [9]. Hence the relations

$$d\tau/dZ = a - d,$$
$$dX_F/dZ = d, \qquad \text{for } Z > Z_p \qquad (8)$$

are obtained, where $d = b(1 - Z_{st})/(1 - Z_p)$. Equations 7 and 8 provide the necessary matching conditions.

The structure of the flame is influenced by the value of the scalar dissipation rate $\chi = 2[\lambda/(\rho c_p)]|\nabla Z|^2$ [6, 11, 14]. The value of this quantity varies across the flowfield and its value at $Z = Z_p$ denoted here by χ_p affects the inner structure of the flame where all the chemical reactions occur. The quantity χ_p is employed in the definition of the Damkohler number. The strain rate influences the flame structure mainly through its influence on χ_p. Although the value of the critical strain rate at extinction depends on the flowfield the value of χ_p at extinction is relatively insensitive to the flowfield.

THE INNER STRUCTURE

The inner structure is governed by finite rates of the global reactions I, II, and III in the reduced chemical-kinetic mechanism. In the reaction zone, the convective terms in the species and the energy balance equations can be neglected because they are of a lower order in comparison to the diffusive and source terms. Hence the equations governing the inner structure of the flame with $x_i = X_i/L_i$ can be written as [1]

$$(\chi_p/2)d^2x_F/dZ^2 = \omega_I,$$
$$(\chi_p/2)d^2x_{H_2}/dZ^2 = -\omega_I - \omega_{II} + 2\omega_{III},$$
$$(\chi_p/2)d^2x_{CO}/dZ^2 = -\omega_I + \omega_{II},$$
$$d^2(4x_F + x_{H_2} + x_{CO} - 2x_{O_2})/dZ^2 = 0,$$
$$d^2(2x_F + x_{H_2} + x_{H_2O})/dZ^2 = 0,$$
$$d^2(x_F + x_{CO} + x_{CO_2})/dZ^2 = 0,$$
$$d^2(x_F + q_a x_{H_2} + q_b x_{CO} + \tau)/dZ^2 = 0, \qquad (9)$$

where ω_k, k = I, II, and III represent the reaction rates of the global steps of the reduced chemical-kinetic mechanism. The quantities $q_a = Q_{III}/2$ and $q_b = Q_{II} + Q_{III}/2$ where $Q_k = (-\bar{Q}_k)/(-\Delta H)$ and $(-\bar{Q}_k)$ represents the heat release in the global step k. By definition $Q_I + Q_{II} + Q_{III} = 1.0$. The principal reaction rates of the global steps I, II, and III of the reduced chemical-kinetic mechanism are equal to the reaction rates of the elementary steps 11, 10, and 5 and can be written as

$$\omega_I = \rho k_{11} X_H L_F x_F/W_{N_2},$$
$$\omega_{II} = \rho k_{10f} X_{H_2O} X_H L_{CO} \times (x_{CO} - \alpha x_{H_2})/(K_3 W_{N_2} L_{H_2} x_{H_2}),$$
$$\omega_{III} = \rho k_5 C_M X_{O_2} X_H/W_{N_2}, \qquad (10)$$

where $\alpha = K_3 X_{CO_2} L_{H_2}/(K_{10} X_{H_2O} L_{CO})$ and K_{10} is the equilibrium constant for the elementary step 10.

The Fuel-Consumption Layer

The structure of this layer is presumed to be governed primarily by finite rates of the global step I of the reduced chemical-kinetic mechanism. Following previous analyses [1, 2] the

variations in the values of the quantities X_{O_2}, X_{H_2O}, and X_{CO_2} which are of order unity and in the values of the quantities X_{H_2} and X_{CO} which are of order ϵ are neglected. The values of X_{H_2} and X_{CO} at the fuel-consumption layer are denoted by $X_{H_2}{}^0$ and $X_{CO}{}^0$ respectively. Also the influence of temperature variations on the structure is neglected because the relevant activation energies are not large [1, 2]. In order to analyze the structure of this layer the expansions $\delta\zeta = (Z - Z_p)$ and $x_F = d\delta y_F$ are introduced. A plausible definition of δ follows from Eq. 1 and can be written as [1, 2, 6].

$$\delta = k_{1f}{}^0 X_{O_2,p}/\left(k_{11}{}^0 L_F d\right), \tag{11}$$

where the superscript 0 over the rate constants denotes that their values are evaluated at the characteristic temperature of the fuel-consumption layer T^0. If the expansions are introduced into the first relation in Eq. 9 and Eqs. 1, 5, 10, and 11 and the definition

$$D_I = \frac{2\rho^0\left(k_{11}K_1{}^{1/2}K_2{}^{1/2}K_3\right)^0 L_F (X_{O_2,p})^{1/2}\left(X_{H_2}{}^0\right)^{3/2}}{\chi_p W_{N_2} X_{H_2O,p}} \tag{12}$$

is used, then Eqs. 38, 40, and 41 of Ref. 1 are obtained. Here ρ^0 is evaluated using the ideal gas law at $T = T^0$. Solution to the equation governing the structure of the fuel-consumption layer yields [1]

$$\delta^2 D_I = 15/8. \tag{13}$$

Equation 13 relates the scalar dissipation rate to T^0 and $X_{H_2}{}^0$ which will be determined from the following analysis of the oxidation layer.

The Oxidation Layer

The analysis of this layer is performed for large values of the Damkohler number of the global step II in the reduced chemical-kinetic mechanism. In this limit the water-gas shift reaction is in equilibrium and it follows from Eq. 10 that $x_{CO} = \alpha x_{H_2}$. Also in this layer $X_F = 0$ and for simplicity, it is assumed that $q_a \approx q_b = q = 0.33$ [1]. With the use of Eqs. 9, the equations governing the structure of this layer can be written as

$$\begin{aligned} &(\chi_p/2)d^2\left[(1+\alpha)x_{H_2}\right]/dZ^2 = 2\omega_{III}, \\ &d^2\left[q(1+\alpha)x_{H_2} + \tau\right]/dZ^2 = 0. \end{aligned} \tag{14}$$

The quantity α is treated as a constant in this layer with the equilibrium constants appearing in the expression for α evaluated at $T = T^0$ and the concentrations set equal to their values calculated from the outer structure at $Z = Z_p$. The expansions

$$\begin{aligned} &Z - Z_p = \epsilon\eta, \qquad (1+\alpha)x_{H_2} = 2d\epsilon z, \\ &\tau - \tau_p = \epsilon(a\eta - 2dqz), \end{aligned} \tag{15}$$

are introduced, where ϵ is a small parameter and z and η are presumed to be of order unity. With $z \to 0$ as $\eta \to -\infty$ the expansion for τ automatically satisfies the coupling relation of Eq. 14 and the matching conditions to the outer structure given by Eq. 7. The source term ω_{III} shown in Eq. 10 in terms of the expansions shown in Eq. 15 can be rewritten using Eqs. 1 and 5 as

$$\omega_{III} = \epsilon^{3/2} D_{III}\chi_p dz^{3/2}/2, \tag{16}$$

where the ratio $k_5 C_M/k_{1f}$ appearing in the expression for C_H in Eq. 1 is neglected. The quantity D_{III} appearing in Eq. 16 is the characteristic Damkohler number and is given by the expression

$$D_{III} = \frac{2^{5/2} d^{1/2} L_{H_2}^{3/2}\left(\rho k_5 C_M K_1{}^{1/2}K_2{}^{1/2}K_3\right)^0 X_{O_2,p}{}^{3/2}}{\chi_p W_{N_2}(1+\alpha)^{3/2} X_{H_2O,p}}, \tag{17}$$

where the values of the rate constants are evaluated at $T = T^0$ and the values of X_{O_2} and X_{H_2O} are set equal to those calculated from the outer structure at $Z = Z_p$. The small expansion parameter ϵ is chosen such that

$$D_{III}\epsilon^{5/2} = 1. \tag{18}$$

Using Eqs. 16 and 18, the first of Eq. 14 can be written as $d^2z/d\eta^2 = z^{3/2}$. This equation must satisfy the conditions $dz/d\eta = 0$ and $z = 0$ as $\eta \to -\infty$ and the matching condition to the fuel-consumption and the nonequilibrium layers which can be written as $dz/d\eta = 1$ at $\eta = 0$ [1]. A first integration of the differential equation for z yields the value of this quantity at $\eta = 0$ given by the expression

$$z^0 = (5/4)^{2/5}. \tag{19}$$

Equations 15 and 19 overpredict the value x_{H_2} at the fuel-consumption layer. To improve the accuracy of the predictions, nonequilibrium of the water-gas reaction should be taken into account [1]. Following the analysis of the nonequilibrium layer outlined in Ref. 1, it can be shown that the corrected value of x_{H_2} at the fuel-consumption layer is

$$x_{H_2}{}^0 = \frac{2d\epsilon z^0}{1+\alpha} - d\nu, \tag{20}$$

where the quantity ν represents the characteristic thickness of the nonequilibrium layer and is given by the expression

$$\nu = \frac{1-\alpha}{(1+\alpha)^{5/4}}\left[\frac{2^{3/2}d^{1/2}\epsilon^{1/2}(z^0)^{1/2}L_{H_2}{}^{1/2}L_{CO}\left(\rho k_{10f}K_1{}^{1/2}K_2{}^{1/2}\right)^0 X_{O_2,p}{}^{1/2}}{\chi_p W_{N_2}}\right]^{-1/2}. \tag{21}$$

RESULTS AND DISCUSSIONS

The characteristic temperature at the fuel-consumption layer T^0 can be calculated by rewriting Eq. 13 with the use of Eqs. 11, 12, 15, 17, 18 and 20 as

$$\frac{\left(k_{1f}{}^0\right)^2 X_{O_2,p}(z^0)^{3/2}}{\epsilon k_5{}^0 C_M^0 k_{11}{}^0 dL_F}\left[1 - \frac{\nu(1+\alpha)}{2\epsilon z^0}\right]^{3/2} = \frac{15}{8}, \tag{22}$$

where it follows from Eqs. 5 and 15 that $\epsilon = (T_p - T^0)/(2\phi_T dqz^0)$. The value of χ_p can be determined by rewriting Eqs. 17 and 18 as

$$\chi_p = \frac{L_{H_2}{}^{3/2}\left(\rho k_5 C_M K_1{}^{1/2}K_2{}^{1/2}K_3\right)^0 X_{O_2,p}{}^{3/2}\left(T_p - T^0\right)^{5/2}}{W_{N_2}d^2q^{5/2}\phi_T{}^{5/2}(z^0)^{5/2}(1+\alpha)^{3/2}X_{H_2O,p}}. \tag{23}$$

Calculations are performed at fixed values of $p = 1$ atm, $Z_{st} = 0.055$ and $T_1 = T_2 = 298$ K. The Lewis numbers are presumed to be constant with $L_F = 0.97$, $L_{H_2} = 0.3$, and $L_{CO} = 1.11$ [1, 2]. Results are obtained for values of $Y_{O_2,2}$ between 0.233 and 0.14 and the value of

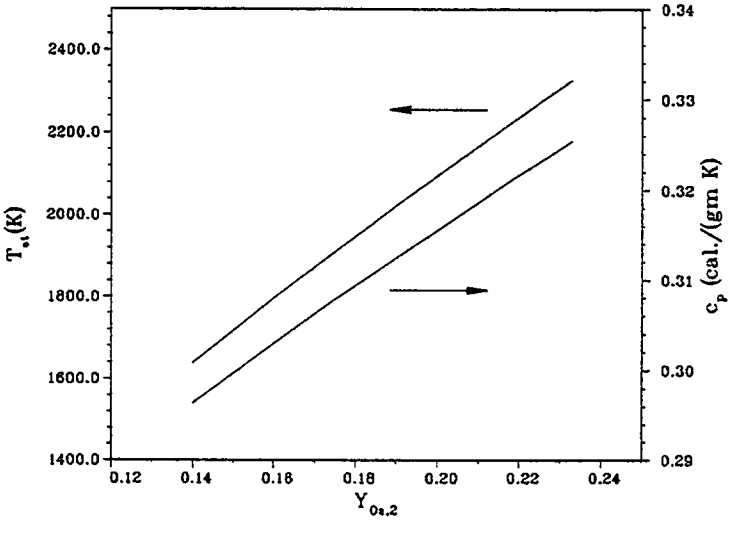

Fig. 2. The adiabatic flame temperature T_{st} and the heat capacity c_p as a function of $Y_{O_2,2}$ for $Z_{st} = 0.055$.

$Y_{F,1}$ is chosen such that the value of Z_{st} is unchanged. The corresponding values of T_{st} and c_p are shown in Fig. 2.

Figures 3 and 4 show the dependence of T^0, T_p, Z_p/Z_{st}, and $X_{O_2,p}$ on χ_p^{-1}, calculated for $Y_{O_2,2} = 0.233$ and $Y_{F,1} = 1.0$ and they all exhibit the classical C-shaped behavior [9, 10]. Stable solutions for T^0, T_p and Z_p/Z_{st} are represented by the upper branch of the C-shaped curve and for $X_{O_2,p}$ by the lower branch. Solutions were not obtained for $\chi_p^{-1} < 0.125$ s; hence it represents the critical value of χ_p at extinction and is denoted here as χ_q. Figure 3 shows the values of T_p and T^0 to decrease with increasing values of χ_p. Figure 4 shows that with increasing values of χ_p the oxygen leakage represented by $X_{O_2,p}$ increases and the value of Z_p/Z_{st} decreases or the flame moves towards the oxidizer stream. These qualitative observations are similar to those found in the previous analysis [1, 2]. Figure 5 shows the value of the scalar dissipation rate at extinction χ_q to decrease with decreasing values of $Y_{O_2,2}$, hence the flame becomes weaker with increasing dilution of the reactant streams. Figure 6 shows the characteristic thickness of the fuel-consumption layer δ, of the nonequilibrium layer ν and of the oxidiation layer ϵ as a function of $Y_{O_2,2}$ at the critical conditions of extinction. The results show that the thickness of the various reaction layers satisfies the presumed ordering $\delta < \nu \ll \epsilon \ll 1$ except at $Y_{O_2,2} = 0.14$ where ν has nearly the same value as δ.

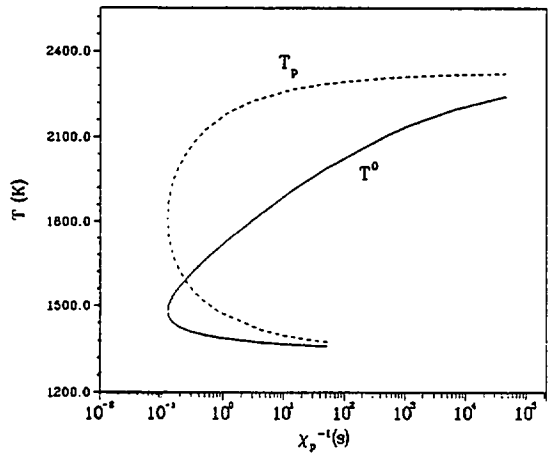

Fig. 3. The dependence of T_p and T^0 on χ_p^{-1} calculated for $Y_{O_2,2} = 0.233$ and $Y_{F,1} = 1.0$.

It is of interest to compare the results obtained using the present model with the predictions of the previous models [1, 2]. In the previous models the scalar dissipation rate at the position where the fuel is consumed [1, 2] appears in the analysis and these models predict its value at extinction. An approximate relation was then employed to calculate the corresponding value of the scalar dissipation rate at $Z = Z_{st}$ [1, 2]. In the present model χ_q represents the value of the scalar dissipation rate at the fuel-consumption layer at extinction. To facilitate comparisons with the previ-

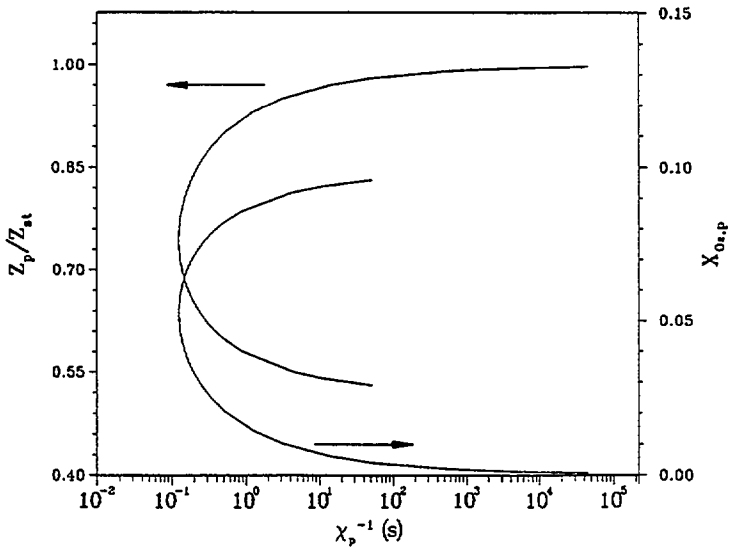

Fig. 4. The dependence of $X_{O_2,p}$ and Z_p/Z_{st} on χ_p^{-1} calculated for $Y_{O_2,2} = 0.233$ and $Y_{F,1} = 1.0$.

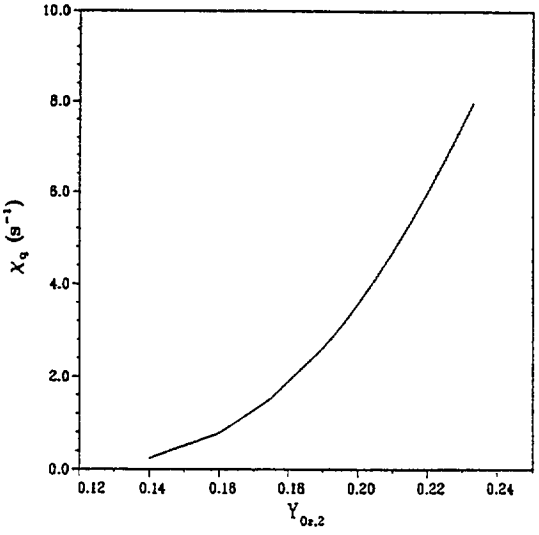

Fig. 5. The scalar dissipation rate at extinction at the fuel-consumption layer χ_q as a function of $Y_{O_2,2}$.

ous models [1, 2], the scalar dissipation rate at extinction at $Z = Z_{st}$ is calculated using the relation $\chi_{st,q} = \chi_q \exp[2(1 - Z_p/Z_{st})]$ [1, 2, 15]. Figures 7–10 show the values of $\chi_{st,q}$, the characteristic temperature at the layer where the fuel is consumed T^0, the oxidizer leakage through the reaction zone and the position of the layer where the fuel is consumed as a

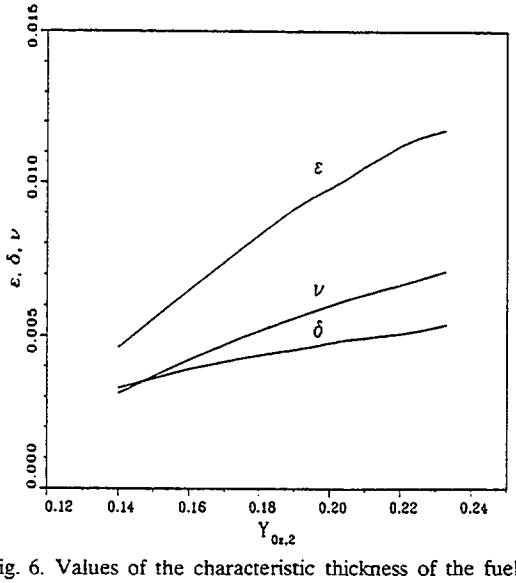

Fig. 6. Values of the characteristic thickness of the fuel-consumption layer δ, the characteristic thickness of the nonequilibrium layer for the global reaction II ν and the characteristic thickness of the oxidation layer ϵ as a function of $Y_{O_2,2}$ at extinction.

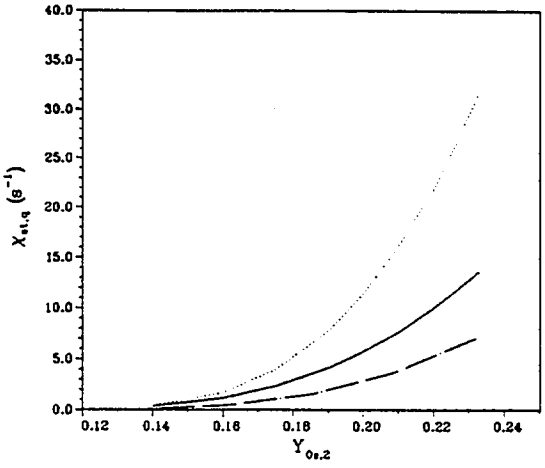

Fig. 7. The scalar dissipation rate at extinction at $Z = Z_{st}$, $\chi_{st,q}$ as a function of $Y_{O_2,2}$. The solid line represents results calculated using the present model, the dotted line represents results calculated using the model of Seshadri and Peters [1] and the chain line represents results obtained by Yang and Seshadri [2] (in the limit $\omega \to \infty$).

function of $Y_{O_2,2}$ at extinction. In these figures the solid lines represent results calculated using the present model, the dotted lines represent results calculated using the asymptotic model of Seshadri and Peters [1] and the chain lines represent results obtained by Yang and Seshadri [2] (in the limit $\omega \to \infty$). Seshadri and Peters [1] had reported results only for $Y_{O_2,2} = 0.233$. Hence the results of their analysis [1] were used to calculate the values of these quantities as a function of $Y_{O_2,2}$ using the rate data shown here. In the analysis of Yang and Seshadri [2] the layer where fuel is consumed is called the inner layer. In this layer and in the oxidation layer the influence of a number of additional reactions were included [2]. Also, water-gas equilibrium was not imposed in the oxidation layer.

Figure 7 shows comparisons between the values of $\chi_{st,q}$ calculated using the various models. The prediction $\chi_{st,q} = 13.42$ s^{-1} at $Y_{O_2,2} = 0.233$ by the present model lies between the values of 31.83 s^{-1} calculated using the model of Seshadri and Peters [1] and the value of 7.04 s^{-1} obtained from the more accurate model of Yang and Seshadri [2]. It is interesting to note that the prediction of the present model agrees very well with the value $\chi_{st,q} = 14.70$ s^{-1} obtained by Chelliah et al. [16] for $Y_{O_2,2} = 0.233$ and $Z_{st} = 0.055$ from

numerical calculations employing a detailed chemical-kinetic mechanism. Figure 7 shows that all models predict the values of $\chi_{st,q}$ to decrease with increasing dilution of the reactant streams and the agreement between the models improves with decreasing values of $Y_{O_2,2}$.

Figure 8 shows the values of T_p calculated using the present model and the values of T^0 predicted by the various models as a function of $Y_{O_2,2}$. The values of T_p and T^0 decrease with decreasing values of $Y_{O_2,2}$ and the values of T^0 predicted by the present model are lower than those predicted by the previous models [1, 2]. Figure 9 shows comparison between the values of $X_{O_2,p}$ calculated by the present model and the values of $X_{O_2}{}^0$ obtained from the previous models [1, 2]. These quantities represent the amount of oxygen leaking through the reaction zone. In the previous models [1, 2] $X_{O_2}{}^0$ was the amount of oxygen in the region where the fuel is consumed. It is interesting that although $X_{O_2}{}^0$ was assumed to be of order ϵ and $X_{O_2,p}$ of order unity, the numerical value of $X_{O_2}{}^0$ is slightly larger than that of $X_{O_2,p}$. From Figs. 6 and 9 it can be observed that the value of $X_{O_2,p}$ is considerably larger than the value of ϵ for all values of $Y_{O_2,2}$ and at $Y_{O_2,2} = 0.233$ the value of $X_{O_2,p}$ is roughly four times larger than the value of

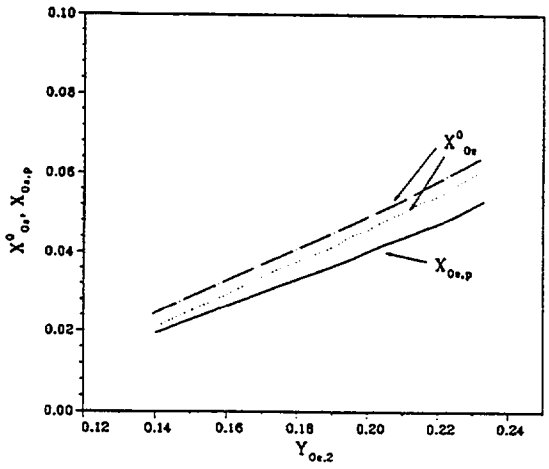

Fig. 9. The characteristic oxidizer leakage as a function of $Y_{O_2,2}$ at extinction. The solid line represents results for $X_{O_2,p}$ calculated using the present model, the dotted line represents results for $X_{O_2}{}^0$ calculated using the model of Seshadri and Peters [1] and the chain line represents results for $X_{O_2}{}^0$ obtained by Yang and Seshadri [2] (in the limit $\omega \to \infty$).

ϵ. Therefore it is justified to treat $X_{O_2,p}$ as a quantity of order unity. At $Y_{O_2,2} = 0.233$ the previous models [1, 2] predict the value of $X_{O_2}{}^0$ to be roughly three times larger than the value of ϵ at conditions close to flame extinction, therefore there is some inaccuracy in treating $X_{O_2}{}^0$ as a quantity of order ϵ. Figure 9 shows

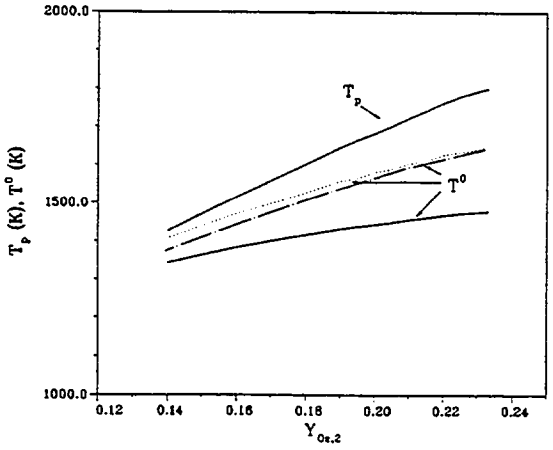

Fig. 8. Values of T_p and T^0 as a function of $Y_{O_2,2}$ at extinction. The solid lines represent results calculated using the present model, the dotted line represents results calculated using the model of Seshadri and Peters [1] and the chain line represents results obtained by Yang and Seshadri [2] (in the limit $\omega \to \infty$).

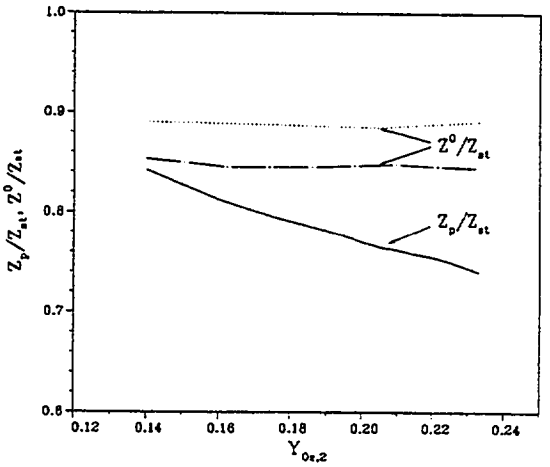

Fig. 10. The position where the fuel is consumed as a function of $Y_{O_2,2}$ at extinction. The solid line represents results for Z_p/Z_{st} calculated using the present model, the dotted line represents results for Z^0/Z_{st} calculated using the model of Seshadri and Peters [1] and the chain line represents results for Z^0/Z_{st} obtained by Yang and Seshadri [2] (in the limit $\omega \to \infty$).

that all models predict the level of oxidizer leakage through the reaction zone to decrease with increasing dilution of the reactant streams.

Finally Fig. 10 shows the value of Z_p to increase slightly with increasing dilution of the reactant streams. Therefore the position of the fuel-consumption layer moves toward the fuel stream with increasing dilution of the reactant streams. The quantity Z^0 shown in Fig. 10 is the position of the fuel-consumption layer and the inner layer respectively in the models of Seshadri and Peters [1] and Yang and Seshadri [2]. Figure 10 shows that the value of Z^0 is relatively insensitive to the level of dilution of the reactant streams.

SUMMARY AND CONCLUSIONS

An asymptotic analysis is performed to predict the structure and critical conditions of extinction of methane–air diffusion flames. The present analysis differs from the previous asymptotic analysis of Seshadri and Peters [1] and Yang and Seshadri [2] in that oxygen is presumed to leak through the reaction zone to the leading order. This approximation considerably simplifies the present analysis and numerical estimates of the amount of oxygen in the reaction zone, calculated using the results of the present model, show that this approximation is reasonably accurate. The predictions of the critical conditions of flame extinction of the present model agree reasonably well with the results of previous numerical calculations using a detailed chemical-kinetic mechanism [16] and fall between the predictions of the previous models [1, 2]. Also a number of qualitative observations of the present model concerning the flame structure are similar to those found from the results of the previous asymptotic analysis [1, 2]. It is anticipated that the present simple model can be used to resolve other relatively complex problems such as pollutant formation in flames and chemical inhibition of flames.

The authors especially wish to thank Professor F. A. Williams for many helpful suggestions and discussions. This work was supported by NIST Grant Number 60NANB3D1435.

REFERENCES

1. Seshadri, K., and Peters, N., *Combust. Flame* 73:23–44 (1988).
2. Yang, B., and Seshadri, K., *Combust. Sci. Technol.* 88:115–132 (1992).
3. Trevino, C., and Williams, F. A., *Prog. Astronaut. Aeronaut.* 113:129–165 (1988).
4. Chelliah, H. K., and Williams, F. A., *Combust. Flame* 80:17–48 (1990).
5. Chelliah, H. K., Trevino, C., and Williams, F. A., *Lect. Notes Phys.* 384:137–158 (1991).
6. Seshadri, K., and Williams, F. A., in *Turbulent Reacting Flows* (P. A. Libby and F. A. Williams, Eds.), Academic, 1994, pp. 153–210.
7. Smooke, M. D., Puri, I. K., and Seshadri, K., *Twenty-First Symposium (International) on Combustion*, The Combustion Institute, Pittsburgh, 1986, pp. 1783–1792.
8. Puri, I. K., Seshadri, K., Smooke, M. D., and Keyes, D. E., *Combust. Sci. Technol.* 56:1–22 (1987).
9. Linan, A., *Acta Astronaut.* 1:1007–1039 (1974).
10. Williams, F. A., *Combustion Theory*, 2nd ed., Addison-Wesley, Redwood City, CA, 1985.
11. Peters, N., and Rogg, B., *Lect. Notes Physics* 15 (1993).
12. Chelliah, H. K., Seshadri, K., and Law, C. K., *Lect. Notes Phys.* 15:224–240 (1993).
13. Peters, N., *Lect. Notes Phys.* 384:48–65 (1991).
14. Peters, N., *Combust. Sci. Technol.* 30:1–17 (1983).
15. Peters, N., *Prog. Ener. Combust. Sci.* 10:319–339 (1984).
16. Chelliah, H. K., Law, C. K., Ueda, T., Smooke, M. D., and Williams, F. A., *Twenty-Third Symposium (International) on Combustion*, The Combustion Institute, Pittsburgh, 1990, pp. 503–511.

Received 28 February 1994; revised 5 July 1994

CHAPTER 2

The Asymptotic Structure of Inhibited Nonpremixed Methane–Air Flames

K. SESHADRI* and N. ILINCIC

Center for Energy and Combustion Research, Department of Applied Mechanics and Engineering Sciences, University of California at San Diego, La Jolla, CA 92093-0411

An asymptotic analysis is performed to determine the influence of CF_3Br on the structure and extinction of nonpremixed methane–air flames. The inhibitor CF_3Br is added to the air-stream of the diffusion flame. A reduced four-step mechanism is used to describe the chemistry taking place in the reaction zone. The outer structure of the flame, in the limit where the rates of the chemical reactions are infinitely fast, is found to consist of two infinitely thin nonpremixed reaction zones which are separated by a chemically inert region. Previous analysis has shown that these reaction zones must merge at conditions close to extinction. Therefore only the asymptotic structure of the merged flame is analyzed here. In the inner structure of the merged flame chemical reactions are presumed to take place in three distinct layers which are identified as the "fuel-consumption-layer," the "oxidation layer" and the "CF_3Br-consumption layer."

The asymptotic analysis predicts the value of the scalar dissipation rate at extinction to decrease and the corresponding value of the maximum flame to increase, with increasing concentration of CF_3Br in the oxidizing stream. However the inhibiting effect of CF_3Br predicted by the asymptotic model is found to be weaker than that measured previously. The differences between the predictions of the asymptotic model and the measurements are attributed to the neglect of inhibition chemistry in the oxidation layer.

INTRODUCTION

A number of experimental, numerical and analytical studies [1–6] have addressed chemical inhibition of flames by bromotrifluoromethane (CF_3Br) because this agent has been found to be very efficient in quenching unwanted fires. However the mechanisms of inhibition of flames by this agent are not clearly understood. Recently restrictions have been placed on the manufacture and use of CF_3Br because this agent is found to contribute to the depletion of ozone in the stratosphere. A search is in progress to identify inhibiting agents that are not harmful to the ozone in the stratosphere but are effective in quenching unwanted fires. Here, the mechanisms of chemical inhibition of counterflow methane–air flames by CF_3Br is addressed with the hope that the knowledge could be used in the search for suitable alternate inhibiting agents. Asymptotic analysis using reduced chemistry is performed to predict the influence of CF_3Br on the structure and critical conditions of extinction of nonpremixed methane–air flames and the results are compared with previous measurements [3].

For uninhibited nonpremixed methane–air flames detailed chemical-kinetic mechanisms have been proposed for predicting their structure and critical conditions of extinction [7]. Also, for these flames reduced five-step and four-step chemical-kinetic mechanisms have been proposed. The structure and critical conditions of extinction obtained from numerical calculations using detailed and reduced chemistry were found to agree reasonably well [8]. Rate-ratio asymptotic analyses using reduced three-step [9–11] and four-step [11, 12] chemical-kinetic mechanisms have been successfully employed previously to predict the critical conditions of extinction of these flames. The techniques employed in these asymptotic analyses are fundamentally different. The analyses of Seshadri and Peters [9] and Yang and Seshadri [12] assumed that fuel is completely consumed in the reaction zone to the leading order and the oxygen leakage through the reaction zone is of order ϵ, where ϵ is the characteristic thickness of an asymptotically thin reaction layer in which a major fraction of the products are formed. However at conditions close to

*Corresponding author.

COMBUSTION AND FLAME 101: 271–294 (1995)

Published by Elsevier Science Inc.

0010-2180/95/$9.50
SSDI 0010-2180(94)00212-B

flame extinction results of asymptotic analyses [9, 12] as well as measurements of the flame structure [13, 14] show significant leakage of oxygen through the reaction zone. In view of these observations an alternative analysis of the flame structure was performed with complete consumption of fuel in the reaction zone and with oxygen leakage from the reaction zone to the leading order [10]. This analysis is simpler and a better representation of the flame structure in the vicinity of the critical conditions of extinction [10], especially for inhibited flames because of enhanced leakage of oxygen through the reaction zone in the presence of the inhibitor. Therefore the techniques developed by Seshadri and Ilincic [10] for analyzing the structure of uninhibited flames are extended here to inhibited methane–air flames.

Milne et al. [3] have performed experiments on inhibited, laminar counterflow diffusion flames stabilized in the forward stagnation region of a porous cylinder. The fuels employed in the study were methane, propane, and *n*-butane. Measurements were made of the minimum concentration of CF_3Br required in the air-stream or in the fuel-stream to extinguish the flame. It was found that CF_3Br was considerably more effective than the inert agents N_2, CO_2, or Ar in extinguishing the flame [3]. In the present study, only the influence on the flame structure arising from addition of CF_3Br to the air-stream is considered.

Hamins et al. [15] performed an experimental and numerical study to elucidate the influence of CF_3Br on the structure and mechanisms of extinction of diffusion flames burning heptane. This study was performed with the inhibitor added to the oxidizer stream [15]. The experimental results showed CF_3Br to be considerably more effective than N_2 in extinguishing the flame [15]. The results of numerical calculations using detailed chemistry showed that the fuel and the inhibitor CF_3Br were consumed in two separate regions of the flame which were referred to as the "fuel-consumption zone," and the "CF_3Br-consumption zone," respectively [15]. The region between these zones was referred to as the "product-formation zone" [15]. The predominant reactions in the fuel-consumption zone were found to be those between the fuel and the radicals and in the CF_3Br-consumption zone those between CF_3Br and the radicals [15]. Hence the CF_3Br-consumption zone is a sink for radicals and this could be responsible for flame inhibition [15]. The concentration of CF_3Br in the fuel-consumption zone was negligibly small as was the concentration of fuel in the CF_3Br-consumption zone [15]. These qualitative observations of the flame structure are also consistent with experimental measurements of the structure of heptane–air diffusion flames inhibited with CF_3Br [16]. Since the asymptotic structures of uninhibited heptane–air diffusion flames and uninhibited methane–air diffusion flames are similar [11], the qualitative features of the structure of inhibited methane–air diffusion flame can be expected to be similar to

TABLE 1

Elementary Reactions and Associated Rate Data Used in the Asymptotic Analysis

No.	Reaction	B_n (mole, cm^3, s)	α_n	E_n (kJ/mole)
1f	$O_2 + H - OH + O$	2.000E + 14	0.00	70.30
1b	$OH + O - O_2 + H$	1.568E + 13	0.00	3.52
2f	$H_2 + O - OH + H$	5.060E + 04	2.67	26.30
2b	$OH + H - H_2 + O$	2.222E + 04	2.67	18.29
3f	$H_2 + OH - H_2O + H$	1.000E + 08	1.60	13.80
3b	$H_2O + H - H_2 + OH$	4.312E + 08	1.60	76.46
4f	$CO + OH - CO_2 + H$	4.400E + 06	1.50	−3.10
4b	$CO_2 + H - CO + OH$	4.956E + 08	1.50	89.76
5	$O_2 + H + M - HO_2 + M$	2.300E + 18	−0.80	0.0
6	$CH_4 + H - CH_3 + H_2$	2.200E + 04	3.00	36.60
7	$H + CF_3Br - CF_3 + HBr$	2.188E + 14	0.00	39.58

that of the inhibited heptane–air diffusion flame. Therefore the results of this previous numerical study of inhibited heptane–air diffusion flames [15] are used as a guide for the following asymptotic analysis.

REDUCED CHEMICAL–KINETIC MECHANISM

Peters [17] has outlined a systematic procedure for deducing reduced chemical–kinetic mechanisms from detailed mechanisms. Table 1 shows the elementary reactions which are presumed to be the principal contributors to the rates of the overall steps of the reduced chemical–kinetic mechanism used in the asymptotic analysis. The reaction rate coefficient k_n of these principal reactions is calculated using the expression $k_n = B_n T^{\alpha_n} \exp[-E_n/(\hat{R}T)]$, where T denotes the temperature and $\hat{R}$ is the universal gas constant. The quantities B_n, α_n, and E_n are the frequency factor, the temperature exponent, and the activation energy, respectively, of the elementary reaction n. In the following asymptotic analysis it is not necessary to resolve the structure of the CF_3Br-consumption zone to determine the critical conditions of extinction. Therefore the rate data for the elementary reaction 7 is not shown in Table 1. The rate data for the elementary steps 1–6 shown in Table 1 are those recommended by Peters and Rogg [7].

For uninhibited methane–air flames the principal path of oxidation is found to be $CH_4 \rightarrow CH_3 \rightarrow CH_2O \rightarrow HCO \rightarrow CO$, $H_2 \rightarrow CO_2, H_2O$ [8]. The radicals H, OH, and O, the unstable species HO_2 and the stable species O_2 participate in chemical reactions along this principal path. Steady-state approximations are introduced for the species CH_3, CH_2O, HCO, OH, O, and HO_2 and they are used to eliminate, respectively, the reaction rates of the elementary steps $CH_3 + O \rightleftharpoons CH_2O + H$, $CH_2O + H \rightleftharpoons HCO + H_2$, $HCO + M \rightleftharpoons H + CO + M$, $H_2 + OH \rightleftharpoons H_2O + H$, $H_2 + O \rightleftharpoons OH + H$, and $HO_2 + H \rightleftharpoons H_2 + O_2$ from the balance equation for the remaining species along the principal path [8, 17]. Starting from the elementary reactions 6, 4, 5, and 1 and using these steady-state approximations the following overall steps

$$CH_4 + 2H + H_2O \rightarrow CO + 4H_2, \qquad (I')$$

$$CO + H_2O \rightleftharpoons CO_2 + H_2, \qquad (II')$$

$$H + H + M \rightarrow H_2 + M, \qquad (III')$$

$$O_2 + 3H_2 \rightleftharpoons 2H + 2H_2O, \qquad (IV')$$

are obtained [8, 17], where M represents any third body. The overall reaction I′ is effectively a chain-breaking step and represent the reaction between the fuel and the radicals to form the intermediate products CO and H_2. The overall reaction II′ represents the oxidation of CO to form the final product CO_2. The overall reaction III′ represents the three-body recombination steps and is also responsible for a major fraction of heat released in the flame. The overall reaction IV′ represents the chain-branching steps. For simplicity the overall steps I′ and III′ are presumed to be irreversible [9, 10].

Westbrook [5] has proposed a detailed chemical–kinetic mechanism for describing the influence of CF_3Br on the structure of premixed flames of hydrogen, methane, methanol and ethene. This mechanism was also employed by Hamins et al. [15] to predict the influence of CF_3Br on heptane–air flames. The results of the previous numerical calculations [15] show that the principal path of decomposition of CF_3Br is $CF_3Br \rightarrow CF_3$, $HBr \rightarrow CF_2O \rightarrow FCO$, $HF \rightarrow CO$. The stable species H_2O, H_2, and F_2 and the radicals F, H, OH, and O participate in chemical reactions along this principal path. In addition to introducing steady-state approximations for the radicals OH and O, steady-state approximations are also introduced for CF_3, CF_2O, FCO, F_2, and F and they are used to eliminate, respectively, the reaction rates of the elementary steps $CF_3 + O \rightleftharpoons CF_2O + F$, $CF_2O + H \rightleftharpoons FCO + HF$, $FCO + M \rightleftharpoons F + CO + M$, $F_2 + H \rightleftharpoons HF + F$, and $F + F + M \rightarrow F_2 + M$ from the balance equation for the remaining species along the principal path [17]. Starting from the elementary reactions 1 and 7 and using these steady-state approximations the overall steps

IV′ and

$$CF_3Br + 6H + H_2O \rightarrow HBr + 3HF + 2H_2 + CO \qquad (V')$$

are obtained [17]. Again, for simplicity the overall step V′ is presumed to be irreversible. The overall step V′ is a net chain-breaking step because it consumes six radicals and forms relatively stable compounds and the chain-breaking effect of CF_3Br is greater than that of CH_4 because only two radicals are consumed in the overall step I′. This chain-breaking effect of CF_3Br is responsible for the chemical-inhibition of the flame. Also it is noteworthy that O_2 does not directly participate in the decomposition of CF_3Br.

The reaction rates w_k, k = I′, II′, III′, IV′, and V′, of the overall steps of the five-step reduced chemical–kinetic mechanism are related to the rates of elementary reactions describing the structure of the inhibited flame. For simplicity, following previous analyses [9, 10] only the rates of the principal elementary steps are used to calculate the rates of the overall steps. Thus

$$\left.\begin{aligned} &w_{I'} = w_6, \quad w_{II'} = w_{4f} - w_{4b}, \\ &w_{III'} = w_5, \quad w_{IV'} = w_{1f} - w_{1b}, \\ &w_{V'} = w_7, \end{aligned}\right\} \qquad (1)$$

where w_n represents the reaction rate of the elementary step n shown in Table 1. The subscripts f and b refer to the forward and backward rate of any elementary step n.

To further simplify the analysis the H-radicals are also presumed to be in steady-state. If the reaction rate of the elementary step 1 or the overall step IV′ is eliminated from the balance equation for the remaining species in the five-step mechanism I′–V′ using the steady-state approximation for H, then the four-step mechanism

$$CH_4 + O_2 \rightarrow CO + H_2 + H_2O, \qquad (I)$$

$$CO + H_2O \rightleftharpoons CO_2 + H_2, \qquad (II)$$

$$O_2 + 2H_2 \rightarrow 2H_2O, \qquad (III)$$

$$CF_3Br + 7H_2 + 3O_2 \rightarrow 5H_2O + HBr + 3HF + CO, \qquad (V)$$

is obtained. The overall steps I, II, and III of this four-step chemical–kinetic mechanism are identical to those used in previous asymptotic analyses of uninhibited methane flames [9, 10]. It is interesting to note that H_2 and O_2 are consumed in the overall step V. The rates of the reduced four-step mechanism are

$$w_I = w_{I'}, \quad w_{II} = w_{II'}, \quad w_{III} = w_{III'}, \quad w_V = w_{V'}. \qquad (2)$$

The reduced four-step chemical–kinetic mechanism consisting of the overall steps I, II, III, and V is used in the asymptotic analysis. The reaction rates of the reduced chemical–kinetic mechanism contain the concentration of the radicals OH, O, and H. Therefore it is necessary to determine the concentrations of these radicals in terms of the concentrations of the species appearing in the four-step mechanism I, II, III, and V. Following previous asymptotic analyses [9, 10] partial-equilibrium assumptions for the elementary steps 3 and 2 are used to express the concentration of OH and O in terms of the concentration of H which can be written as

$$C_{OH} = C_H C_{H_2O}/(K_3 C_{H_2}),$$
$$C_O = C_{H_2O} C_H{}^2/\left(K_2 K_3 C_{H_2}{}^2\right), \qquad (3)$$

where C_i denotes the concentration of species i and K_n is the equilibrium constant for the elementary step n. Steady-state approximation for H implies that $w_{I'} + w_{III'} + 3w_{V'} = w_{IV'}$. Using the principal rates for the four-step reduced chemical–kinetic mechanism the concentration of H can be calculated from the expression

$$C_H = \frac{K_1{}^{1/2} K_2{}^{1/2} K_3 C_{H_2}{}^{3/2} C_{O_2}{}^{1/2}}{C_{H_2O}} \times \left[1 - \frac{k_5 C_M}{k_{1f}} - \frac{k_6 C_F}{k_{1f} C_{O_2}} - \frac{3k_7 C_I}{k_{1f} C_{O_2}}\right]. \qquad (4)$$

The concentration of the third body C_M is calculated using the relation $C_M = [p\overline{W}/(\hat{R}T)] \sum_{i=1}^{n} \eta_i Y_i / W_i$, where p denotes the pressure, $\overline{W}$ is the average molecular weight and Y_i, η_i, and

W_i are the mass fraction, the Chaperon efficiency and the molecular weight of species i. For simplicity the average molecular weight is presumed to be a constant and only the mass fractions of H_2O, CO_2, and N_2 calculated for stoichiometric combustion of methane and air by a one-step reaction are used to calculate C_M. The values of η_i used here are 6.5, 1.5, and 0.4 for H_2O, CO_2, and N_2 respectively.

THE OUTER STRUCTURE

Figure 1 shows a schematic illustration of the overall outer structure in the limit where the rates of the chemical reactions are infinitely fast [18]. The quantity ξ in Fig. 1 is a conserved scalar [11, 18, 19] and is defined as $\xi = (Z_C - Z_{C,2})/(Z_{C,1} - Z_{C,2})$, where Z_C represents the mass fraction of the element carbon at any location in the flow-field [19] and the subscripts 1 and 2 denote conditions in the ambient fuel stream and the ambient oxidizer stream respectively. It follows from this definition that $\xi = 1.0$ in the ambient fuel stream and $\xi = 0$ in the ambient oxidizer stream. In the limit where the rates of the chemical reactions are infinitely fast, CH_4 and CF_3Br are consumed in different infinitely thin zones located respectively at ξ_p and ξ_l. Fuel is completely consumed to the leading order at ξ_p and the chemistry is represented by the global step

$$CH_4 + 2O_2 \rightarrow CO_2 + 2H_2O. \qquad \text{(GI)}$$

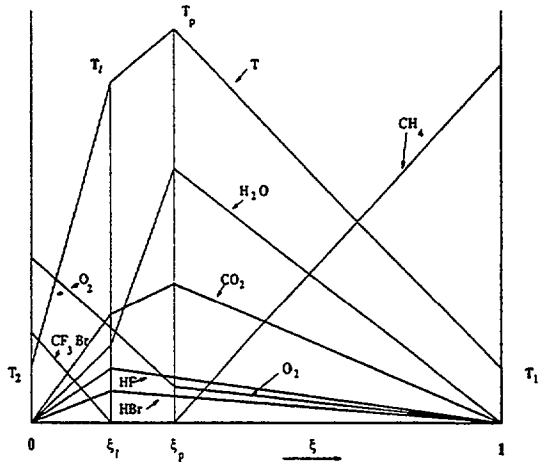

Fig. 1. Schematic illustration of the outer structure.

The global step GI can also be deduced from the overall steps I, II, and III by introducing steady-state approximations for the intermediate species H_2 and CO. At ξ_l, CF_3Br is completely consumed to the leading order and the chemistry is represented by the one-step reaction

$$CF_3Br + 2H_2O \rightarrow HBr + 3HF + CO_2. \qquad \text{(GII)}$$

The global step GII can also be deduced from the overall steps II, III, and V by introducing steady-state approximations for the intermediate species H_2 and CO. It is noteworthy that the global step GII does not involve O_2. It is interesting to compare the outer structure of the flame shown in Fig. 1 with the outer structures of partially premixed flames analyzed by Peters [19] and Hamins et al. [20]. Peters [19] analyzed the structure of counterflow partially premixed flames where both reactant streams contain fuel and oxygen. The activation energy characterizing the one-step chemical reaction between the fuel and oxygen was presumed to be large [19] and the reactions were presumed to occur in a thin nonpremixed flame and in two premixed flames one on each side of this nonpremixed flame [19]. These flames were presumed to be separated by chemically inert regions [19]. Hamins et al. [20], employing large activation energy asymptotic techniques, analyzed the structure of counterflow partially premixed flames where one stream was fuel and the other was a mixture of fuel and oxygen. In this case chemical reactions were presumed to occur in a thin nonpremixed flame and in a premixed flame on the oxidizer side of this nonpremixed flame. These flames were again separated by chemically inert regions. The outer structure shown in Fig. 1 is different from the outer structure of these partially premixed flames [19, 20]. Here the reaction zone located at ξ_p is a nonpremixed flame where chemical reaction between fuel and oxygen takes place as illustrated by the global step GI. Also the reaction zone located at ξ_l is a nonpremixed flame where chemical reaction takes place between CF_3Br and a product formed in the reaction zone located at ξ_p as illustrated by the global

step GII. These reaction zones are again separated by chemically inert regions.

The reactant and product distributions around $\xi = \xi_p$ shown in Fig. 1 are similar to the structure of a nonpremixed flame in the "premixed-flame" regime analyzed by Liñán [21] and to the structure of the uninhibited flame analyzed by Seshadri and Ilincic [10]. Fuel is completely consumed at ξ_p whereas oxygen leaks through the reaction zone into the ambient fuel stream to the leading order. The maximum value of the flame temperature T_p is attained at ξ_p. The gradients of temperature and concentration of CH_4, O_2, CO_2, and H_2O are discontinuous at ξ_p. The region $\xi_p < \xi < 1$ represents frozen flow because both fuel and oxygen coexist in this region. At ξ_l, CF_3Br is completely consumed and the value of the flame temperature is denoted by T_l. Also at this position the gradients of temperature and concentration of CF_3Br, H_2O, CO_2, HF, and HBr are discontinuous but the gradient of O_2 is continuous because oxygen does not participate in the chemical reaction as illustrated by the global step GII. The region $0 < \xi < \xi_l$ represents frozen flow because CF_3Br and H_2O coexist in this region whereas the region $\xi_l < \xi < \xi_p$ represents equilibrium flow.

For simplicity the Lewis numbers $L_i = \lambda/(\rho c_p D_i)$ of the species appearing in the global steps GI and GII are presumed to be equal to unity. Here λ, ρ, and c_p denote the coefficient of thermal conductivity, the density and the heat capacity of the gas mixture respectively and D_i is the coefficient of diffusion of species i. In view of the global step GI the coupling relation between the mass fractions of O_2 and CH_4 can be written as [18–23]

$$\frac{Y_{O_2}}{2W_{O_2}} - \frac{Y_F}{W_F} = \frac{Y_{O_2,2}}{2W_{O_2}}\left[1 - \left(1 + \frac{2Y_{F,1}W_{O_2}}{Y_{O_2,2}W_F}\right)\xi\right], \quad (5)$$

where the subscript F denotes the fuel and the subscripts 1 and 2 denote conditions in the ambient fuel stream and the ambient oxidizer stream respectively. The value of ξ_p at which there is no oxygen leakage through the reaction zone is denoted by ξ_{st} which can be determined from Eq. 5 by setting $Y_F = Y_{O_2} = 0$ and is given by the expression

$$\xi_{st} = \left[1 + 2Y_{F,1}W_{O_2}/(Y_{O_2,2}W_F)\right]^{-1}. \quad (6)$$

Using the stoichiometry of the global steps GI and GII additional expressions relating the mass fractions of H_2O, CO_2, HBr, and HF to the mass fractions of CH_4 and CF_3Br can be written as

$$\left.\begin{aligned} &\frac{Y_{H_2O}}{W_{H_2O}} - 2\frac{Y_I}{W_I} + 2\frac{Y_F}{W_F} \\ &\quad = 2\left(\frac{Y_{F,1}}{W_F} + \frac{Y_{I,2}}{W_I}\right)\xi - 2\frac{Y_{I,2}}{W_I}, \\ &\frac{Y_{CO_2}}{W_{CO_2}} + \frac{Y_I}{W_I} + \frac{Y_F}{W_F} \\ &\quad = \left(\frac{Y_{F,1}}{W_F} - \frac{Y_{I,2}}{W_I}\right)\xi + \frac{Y_{I,2}}{W_I}, \\ &\frac{Y_{HBr}}{W_{HBr}} + \frac{Y_I}{W_I} = \frac{Y_{HF}}{3W_{HF}} + \frac{Y_I}{W_I} \\ &\quad = \frac{Y_{I,2}}{W_I}(1 - \xi), \end{aligned}\right\} \quad (7)$$

where the subscript I denotes the inhibitor. From the first expression in Eq. 7 the minimum value of ξ_l determined by setting $Y_F = Y_I = Y_{H_2O} = 0$ is $(\xi_l)_{min} = [1 + Y_{F,1}W_I/(Y_{I,2}W_F)]^{-1}$. If the heat capacity is presumed to be constant, then the coupling relation between the temperature T and the mass fractions of CH_4 and CF_3Br can be written as

$$c_p[T - T_u(\xi)] = \frac{(-\Delta H_{GI})}{W_F}[Y_{F,1}\xi - Y_F] + \frac{(-\Delta H_{GII})}{W_I}[Y_{I,2}(1 - \xi) - Y_I], \quad (8)$$

where $(-\Delta H_{GI})$ and $(-\Delta H_{GII})$ denote the heat release in the global steps GI and GII, respectively, and $T_u(\xi) = T_2 + (T_1 - T_2)\xi$. At $\xi = \xi_p$ the value of T_p can be determined

from Eq. 8 by setting $Y_F = Y_I = 0$. Thus

$$c_p[T_p - T_u(\xi_p)] = \frac{(-\Delta H_{GI})Y_{F,1}\xi_p}{W_F} + \frac{(-\Delta H_{GII})Y_{I,2}(1-\xi_p)}{W_I}. \quad (9)$$

The maximum value of T_p is achieved when there is no oxygen leakage through the reaction zone and is denoted here by T_{st} which can be determined from Eq. 9 by setting $\xi_p = \xi_{st}$.

For partially premixed flames Peters [19] has shown that the premixed and nonpremixed reaction zones merge at conditions close to extinction. For uninhibited methane–air diffusion flames, the rate-ratio asymptotic analysis of Yang and Seshadri [12] has shown that the effective activation energy of the global step GI is large. If the effective activation energy of the global step GII is also presumed to be large, then in view of the results obtained by Peters [19] the reaction zones at ξ_p and ξ_I can be expected to merge at conditions close to flame extinction. Since the primary focus of the present analysis is to determine the critical conditions of extinction, attention is restricted to the merged structure obtained by setting $\xi_I = \xi_p$ to the leading order. For convenience the definitions [9–12]

$$\left.\begin{aligned} X_i &\equiv \frac{Y_i W_{N_2}}{W_i}, \qquad \tau \equiv \frac{[T - T_u(\xi)]Y_{F,1}W_{N_2}\xi_{st}}{[T_{st} - T_u(\xi_{st})]W_F}, \\ b &\equiv \frac{Y_{O_2,2}W_{N_2}}{2W_{O_2}\xi_{st}}, \qquad c \equiv \frac{Y_{I,2}W_{N_2}}{W_I\xi_{st}}, \\ h &\equiv \frac{1 + c(-\Delta H_{GII})\xi_{st}(1-\xi_p)/[b(-\Delta H_{GI})(1-\xi_{st})\xi_p]}{1 + c(-\Delta H_{GII})/[b(-\Delta H_{GI})]}, \end{aligned}\right\} \quad (10)$$

are introduced. For the merged flame located at ξ_p the amount of oxidizer leakage through the reaction zone and the concentrations of the products deduced from Eqs. 5–7 and 10 by setting $Y_F = Y_I = 0$ are

$$\left.\begin{aligned} X_{O_2,p} &= 2b\xi_{st}(1 - \xi_p/\xi_{st}), \\ X_{H_2O,p} &= 2b(1-\xi_{st})\xi_p - 2c\xi_{st}(1-\xi_p), \\ X_{CO_2,p} &= b(1-\xi_{st})\xi_p + c\xi_{st}(1-\xi_p), \\ X_{HBr,p} &= X_{HF,p}/3 = c\xi_{st}(1-\xi_p). \end{aligned}\right\} \quad (11)$$

For the merged flame the slopes of X_F, τ, X_I, and X_{O_2} deduced from Eqs. 5–8 and 10 in the region $\xi > \xi_p$ are

$$\left.\begin{aligned} \frac{dX_F}{d\xi} &= b\frac{1-\xi_{st}}{1-\xi_p}, \qquad \frac{d\tau}{d\xi} = -bh\xi_p\frac{1-\xi_{st}}{1-\xi_p}, \\ \frac{dX_I}{d\xi} &= 0, \qquad \frac{dX_{O_2}}{d\xi} = -2b\frac{\xi_{st}-\xi_p}{1-\xi_p}. \end{aligned}\right\} \quad (12)$$

For the merged flame the slopes of X_F, τ, X_I, and X_{O_2} deduced from Eqs. 5–8 and 10 in the region $\xi < \xi_p$ are

$$\left.\begin{aligned} \frac{dX_F}{d\xi} &= 0, \qquad \frac{d\tau}{d\xi} = bh(1-\xi_{st}), \\ \frac{dX_I}{d\xi} &= -c\frac{\xi_{st}}{\xi_p}, \qquad \frac{dX_{O_2}}{d\xi} = -2b. \end{aligned}\right\} \quad (13)$$

Equations 12 and 13 provide the appropriate matching conditions between the outer and the inner structures.

The structure of the flame is influenced by the value of the scalar dissipation rate $\chi = 2[\lambda/(\rho c_p)](\nabla\xi)^2$ [18, 19, 22, 23]. The value of χ varies across the flowfield and its value at the inner structure of the merged flame is denoted by χ_p. The strain rate a influences the flame structure mainly through its influence on χ_p.

INNER STRUCTURE

Figure 2 shows a schematic illustration of the profiles of CH_4, CF_3Br, H_2, and H in the inner structure of the merged flame. Chemical reactions are presumed to occur in three distinct layers which are identified as the "fuel-consumption layer" of thickness of order δ, the "oxidation layer" of thickness of order ϵ and the "CF_3Br-consumption layer." In view of the results of previous numerical calculations of the structure of inhibited heptane flame [15], CH_4 and CF_3Br are presumed to be consumed in different regions of the flame and the concentration of CH_4 is presumed to be nonnegligible only in the fuel-consumption layer and the concentration of CF_3Br is presumed to be nonnegligible only in the CF_3Br-consumption layer. The water-gas shift reaction represented by the overall step II is presumed to be in equilibrium everywhere except in a thin nonequilibrium layer of thickness of order ν. The ordering $\delta \ll \nu \ll \epsilon \ll 1$ used in the present analysis is similar to those employed in the previous asymptotic analyses of uninhibited flames [9, 10]. The thickness of the CF_3Br-consumption layer is not marked in Fig. 2 because in the analysis developed here, it is not necessary to resolve the structure of this layer to determine the critical conditions of extinction. The relative location of these layers with respect to one another in terms of η is shown in Fig. 2, where η represents a stretched independent variable used in the analysis of the oxidation layer. The structures of the fuel-consumption layer and the non-equilibrium layer are presumed to be identical to those for the uninhibited methane–air flames analyzed previously [10]. The structure of the oxidation layer of the inhibited flame analyzed here is different from that of the uninhibited flame due to the presence of the CF_3Br-consumption layer which is a radical sink.

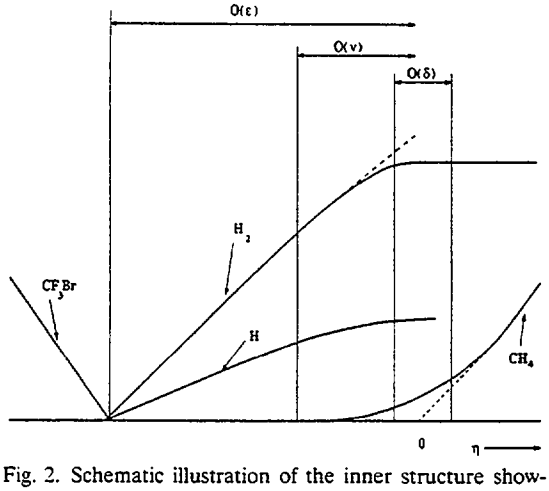

Fig. 2. Schematic illustration of the inner structure showing the fuel-consumption layer, the layer where the global reaction II is not in equilibrium, the oxidation layer and the CF_3Br consumption layer.

In the fuel-consumption layer which is located at ξ_p the fuel reacts with the radicals in accordance with the overall step I to primarily form H_2 and CO and some CO_2 and H_2O [9, 10]. Following previous analysis [10] oxygen is presumed to leak through the fuel-consumption layer to the leading order. The maximum value of the flame temperature is attained at the fuel-consumption layer and is denoted by T^0 and due to finite rates of the chemical reactions its value is less than T_p. The quantity T^0 also represents the characteristic temperature at which the rates of the chemical reactions that take place in the fuel-consumption layer are evaluated. In the oxidation layer the concentrations of CH_4 and CF_3Br are presumed to be zero and in this layer CO and H_2 are oxidized to form CO_2 and H_2O. In the CF_3Br-consumption layer the inhibitor reacts with the radicals to form CO, HBr and HF in accordance with the overall step V.

In the inner structure the convective terms in the species and the energy balance equations can be neglected because they are of a lower order in comparison to the diffusive and the source terms. For convenience the defini-

tions

$$x_i \equiv \frac{X_i}{L_i}, \qquad \omega_k \equiv \frac{W_{N_2} w_k}{\rho},$$

$$Q_k \equiv \frac{(-\Delta H_k)}{(-\Delta H_{GI}) + c(-\Delta H_{GII})/b}, \tag{14}$$

are introduced where $(-\Delta H_k)$ is the heat release in the overall step k of the reduced four-step mechanism. It follows that $Q_I + (1 + c/b)Q_{II} + (1 - 3c/b)Q_{III} + (c/b)Q_V = 1$. The equations governing the inner structure written in terms of the variables defined in Eq. 14 are

$$\left.\begin{aligned}
&(\chi_p/2)d^2x_F/d\xi^2 = \omega_I,\\
&(\chi_p/2)d^2x_{H_2}/d\xi^2\\
&\quad = -\omega_I - \omega_{II} + 2\omega_{III} + 7\omega_V,\\
&(\chi_p/2)d^2x_{CO}/d\xi^2 = -\omega_I + \omega_{II} - \omega_V,\\
&(\chi_p/2)d^2x_I/d\xi^2 = \omega_V,\\
&d^2(x_{H_2} + x_{CO} - 2x_{O_2} + 4x_F)/d\xi^2 = 0,\\
&d^2(x_{H_2O} + x_{H_2} + 2x_F - 2x_I)/d\xi^2 = 0,\\
&d^2(x_{CO_2} + x_{CO} + x_F + x_I)/d\xi^2 = 0,\\
&d^2(x_{HBr} + x_I)/d\xi^2 = 0,\\
&d^2(x_{HF} + 3x_I)/d\xi^2 = 0,\\
&d^2(\tau + q_a x_{H_2} + q_b x_{CO} + q_c x_F + q_d x_I)/\\
&\quad d\xi^2 = 0,
\end{aligned}\right\} \tag{15}$$

where $q_a = Q_{III}/2$, $q_b = Q_{II} + Q_{III}/2$, $q_c = Q_I + Q_{II} + Q_{III}$, and $q_d = Q_{II} - 3Q_{III} + Q_V$. Thermochemical calculations show that the value of Q_{II} is small, thus for simplicity the approximation $q_a \approx q_b \approx q \equiv (Q_{II} + Q_{III})/2$ which was employed in previous asymptotic analyses [9, 10] is also used here.

Fuel-Consumption Layer

The influence of the overall step V on the structure of the fuel-consumption layer can be neglected because the concentration of CF_3Br is negligibly small. Also following previous asymptotic analyses [9, 10] the influence of the overall steps II and III on the structure of the fuel-consumption layer is neglected to the leading order. Thus the structure of this layer is governed primarily by the finite rate of the overall step I. In the fuel-consumption layer the quantities X_{O_2}, X_{H_2O}, and X_{CO_2} are of order unity hence their values are evaluated at ξ_p using Eq. 11. The quantities X_{H_2} and X_{CO} are of order ϵ; hence their values at the fuel-consumption layer which are denoted here by $X_{H_2}{}^0$ and $X_{CO}{}^0$ respectively are evaluated using the results of the asymptotic analysis of the oxidation layer. With these approximations, the equations governing the structure of this layer become identical to those derived previously [9, 10] for the uninhibited methane–air flame and the results of these previous analyses can be written as

$$\frac{2\rho^0\left(k_6 K_1^{1/2} K_2^{1/2} K_3\right)^0 L_F X_{O_2,p}{}^{1/2}\left(X_{H_2}{}^0\right)^{3/2}}{\chi_p W_{N_2} X_{H_2O,p}} = \delta^2 = 15/8, \tag{16}$$

where the superscript 0 over the rate constants and the equilibrium constants denotes that their values are evaluated at the characteristic temperature T^0 of the fuel-consumption layer. Also the quantity ρ^0 is evaluated using the ideal gas law at $T = T^0$. It has been shown previously [9, 10] that the characteristic thickness of the fuel-consumption layer δ can be evaluated from the expression

$$\delta = k_{1f}{}^0 X_{O_2,p}(1 - \xi_p)/\left[k_6{}^0 b L_F (1 - \xi_{st})\right]. \tag{17}$$

Equation 16 relates the scalar dissipation rate to T^0 and $X_{H_2}{}^0$. These quantities will be determined by analyzing the structure of the oxidation layer.

Oxidation Layer

The asymptotic analysis of the oxidation layer is performed with the overall step II of the reduced chemical-kinetic mechanism presumed to be in equilibrium [9, 10], which implies that the elementary reactions 4f and 4b shown in Table 1 are in partial equilibrium. Thus using Eq. 3 the concentration of CO can be related to the concentration of H_2

using the expression $x_{CO} = \alpha x_{H_2}$, where $\alpha = [K_3^0 X_{CO_2,p} L_{H_2}/(K_4^0 X_{H_2O,p} L_{CO})]$ to the leading order and the equilibrium constants appearing in the expression for α are evaluated at T^0. In the oxidation layer the concentrations of fuel and the inhibitor are presumed to be negligibly small, hence the influence of the overall steps I and V on the structure of this layer can be neglected. Introducing these approximations into the second, third, and the last expressions of Eq. 15, the equations

$$\left.\begin{aligned} &(\chi_p/2) d^2[(1+\alpha)x_{H_2}]/d\xi^2 \\ &\quad = 2\omega_{III} = 2\rho^0 k_5^0 C_M^0 X_{O_2,p} X_H / W_{N_2}, \\ &d^2[\tau + q(1+\alpha)x_{H_2}]/d\xi^2 = 0 \end{aligned}\right\} \tag{18}$$

are obtained, where the values of the density, the concentration of the third body and the rate parameters are evaluated at T^0 and their variations with temperature are considered to be negligibly small [9, 10]. The expansions

$$\xi - \xi_p = \epsilon\eta,$$

$$(1+\alpha)x_{H_2} = 2b(1-\xi_{st})\epsilon z/(1-\xi_p),$$

$$\tau - \tau_p = \epsilon t, \tag{19}$$

are introduced, where ϵ is a small parameter and a measure of the thickness of the oxidation layer and z, t, and η are of order unity. A relation between t and z can be obtained by integrating the last expression of Eq. 15 once across the fuel-consumption layer where $\omega_V = 0$ and matching the result with the gradients of τ and X_F shown in Eq. 12. This gives the result $d[\tau + q(1+\alpha)x_{H_2}]/d\xi = b(1-\xi_{st}) - cq_d$ in the oxidation layer. This result can also be obtained by integrating the last expression of Eq. 15 across the CF_3Br-consumption layer where $\omega_I = 0$ and matching the result with the gradients of τ and X_I shown in Eq. 13. If the expansions shown in Eq. 19 are introduced into this expression and integrated, the result $t = [b(1-\xi_{st}) - cq_d]\eta - 2bq(1-\xi_{st})z/(1-\xi_p)$ is obtained, where the constant of integration is set equal to zero. The value of X_H appearing in Eq. 18 can be evaluated using Eqs. 4, 10, 14, and 19 which gives to the leading order

$$X_H = \frac{\epsilon^{3/2} 2^{3/2} b^{3/2} (1-\xi_{st})^{3/2} \left(K_1^{1/2} K_2^{1/2} K_3\right)^0 L_{H_2}^{3/2} X_{O_2,p}^{1/2}}{(1+\alpha)^{3/2}(1-\xi_p)^{3/2} X_{H_2O,p}} z^{3/2}, \tag{20}$$

where the term $k_5 C_M / k_{1f}$ appearing in Eq. 4 is neglected because it is small in comparison to unity [11].

If the small expansion parameter ϵ is chosen such that

$$\epsilon^{-5/2} = \frac{2^{5/2} b^{1/2} (1-\xi_{st})^{1/2} \left(\rho k_5 C_M K_1^{1/2} K_2^{1/2} K_3\right)^0 L_{H_2}^{3/2} X_{O_2,p}^{3/2}}{\chi_p (1+\alpha)^{3/2}(1-\xi_p)^{1/2} W_{N_2} X_{H_2O,p}}, \tag{21}$$

then from Eqs. 18–21 the differential equation

$$d^2 z/d\eta^2 = z^{3/2}, \tag{22}$$

is obtained. Boundary conditions for Eq. 22 must be obtained by matching the solutions in the oxidation layer with those in the fuel-consumption and the CF_3Br-consumption layers. If the influence of the overall steps III and V on the structure of the fuel-consumption layer is neglected then from Eq. 15 the coupling relation $d^2(x_{H_2} + x_{CO} + 2x_F)/d\xi^2 = 0$ is obtained. Integrating this expression once and matching the result with the outer solution in the inert region $\xi > \xi_p$ shown by Eq. 12 the result $d(x_{H_2} + x_{CO} + 2x_F)/d\xi = 2b(1-\xi_{st})/(1-\xi_p)$ is obtained. Matching this result with the solution in the oxidation layer and

using the expansions shown in Eq. 19 gives the boundary condition $dz/d\eta = 1$ at $\eta = 0$.

If the influence of the overall steps I and III on the structure of the CF_3Br-consumption layer is neglected then from Eq. 15 the coupling relation $d^2(x_{H_2} + x_{CO} - 6x_f)/d\xi^2 = 0$ is obtained. Integrating this expression once and matching the result with the outer solution in the inert region $\xi < \xi_p$ shown by Eq. 13 the result $d(x_{H_2} + x_{CO} - 6x_f)/d\xi = 6c\xi_{st}/\xi_p$ is obtained. Matching this result with the solution in the oxidation layer and using the expansions shown in Eq. 19 yields the boundary condition $dz/d\eta = 3(c/b)\xi_{st}(1 - \xi_p)/[\xi_p(1 - \xi_{st})]$ at $\eta = \eta_l \equiv (\xi_l - \xi_p)/\epsilon$. In addition at $\eta = \eta_l$ the concentration of H_2 is zero to the leading order which implies that $z = 0$ at η_l. Integrating Eq. 22 once and using the boundary conditions at $\eta = 0$ and $\eta = \eta_l$ gives

$$z^0 = \left[\frac{5}{4} - \frac{45c^2\xi_{st}^2(1 - \xi_p)^2}{4b^2\xi_p^2(1 - \xi_{st})^2}\right]^{2/5}, \tag{23}$$

where z^0 is the value of z at $\eta = 0$. Equations 19 and 23 can be used to calculate the value of $x_{H_2}^0$ at the fuel-consumption layer. Previous studies have shown [9, 10] that the presence of the non-equilibrium layer for the water-gas shift reaction adjacent to the fuel-consumption layer introduces significant corrections to the value of $x_{H_2}^0$ and the corrected value of this quantity is given by the expression

$$x_{H_2}^0 = 2\epsilon bz^0(1 - \xi_{st})/[(1 + \alpha)(1 - \xi_p)] - \nu b(1 - \xi_{st})/(1 - \xi_p), \tag{24}$$

where the quantity ν represents the characteristic thickness of the nonequilibrium layer and is given by the expression [9, 10]

$$\nu = \frac{\epsilon(1 - \alpha)}{(z^0)^{1/4}(1 + \alpha)^2} \times \left[\frac{2k_5^0 C_M^0 K_3^0 L_{H_2} X_{O_2,p}}{L_{CO} k_{4f}^0 X_{H_2O,p}}\right]^{1/2}. \tag{25}$$

An equation for calculating the characteristic temperature at the fuel-consumption layer can be obtained by eliminating χ_p from Eqs. 16 and 21 and also using Eqs. 17 and 24 which gives the expression

$$\frac{(k_{1f}^0)^2(1 - \xi_p)X_{O_2,p}(z^0)^{3/2}}{\epsilon b k_5^0 C_M^0 k_6^0 L_F(1 - \xi_{st})} \times \left[1 - \frac{\nu(1 + \alpha)}{2\epsilon z^0}\right]^{3/2} = \frac{15}{8}. \tag{26}$$

Using Eqs. 19, 6, and 10 the quantity ϵ appearing in Eq. 26 can be related to T^0 as

$$\epsilon = \frac{(T_p - T^0)(1 - \xi_p)\xi_{st}}{2qz^0[T_{st} - T_u(\xi_{st})]}. \tag{27}$$

The value of χ_p can be obtained by rewriting Eq. 21 and using Eq. 27 which gives the result

$$\chi_p = \frac{b^{1/2}(1 - \xi_p)^2(1 - \xi_{st})^{1/2}\xi_{st}^{5/2}\left(\rho k_5 C_M K_1^{1/2} K_2^{1/2} K_3\right)^0 L_{H_2}^{3/2} X_{O_2,p}^{3/2}(T_p - T^0)^{5/2}}{q^{5/2}(z^0)^{5/2}(1 + \alpha)^{3/2} W_{N_2} X_{H_2O,p}[T_{st} - T_u(\xi_{st})]^{5/2}}. \tag{28}$$

For known composition of the reactant streams and for an appropriate value of c_p Eqs. 6 and 9 are used to calculate ξ_{st} and T_{st}. For a chosen value of ξ_p Eqs. 9–13 are employed to calculate the value of T_p, the concentration of various species and their gradients. Equations 23 and 25–27 are then used to calculate T^0. The value of χ_p corresponding to the chosen value of ξ_p is then calculated using Eq. 28. The results are discussed in the following section.

RESULTS AND DISCUSSIONS

Calculations are performed at fixed values of p = 1 atm, $Y_{F,1}$ = 1.0 and $T_1 = T_2$ = 300 K. The Lewis numbers are presumed to be constant with L_F = 0.97, L_{H_2} = 0.3 and L_{CO} = 1.11 [9–12]. Results are obtained for 0% to 3% CF_3Br by volume in air for which the corresponding values of $Y_{I,2}$ are between 0 and 0.14. For a given composition of the reactant streams all calculations are performed with the value of the heat capacity presumed to be constant. The values of $Y_{I,2}$, $Y_{O_2,2}$, ξ_{st}, T_{st}, c_p, and q used in the calculations are shown in Table 2. For $Y_{I,2}$ = 0.153 and for no leakage of oxygen through the reaction zone, which implies that $\xi_p = \xi_{st}$ (see Eq. 11), the value of z^0 calculated from Eq. 23 is zero. Therefore the asymptotic analysis developed here is not valid for values of $Y_{I,2}$ greater than 0.153.

Figures 3–6 show the values of T_p, T^0, $X_{O_2,p}$ and $(\xi_p - \xi_{st})/\xi_{st}$ as a function of χ_p^{-1} calculated for 0%, 1%, 2%, and 3% CF_3Br by volume in the air-stream or for $Y_{I,2}$ = 0, 0.05, 0.095, and 0.138. The amount of CF_3Br is constant along each curve. All the curves shown in Figs. 3–6 exhibit the classical C-shaped behavior. Stable solutions for T_p, T^0, and $(\xi_p - \xi_{st})/\xi_{st}$ are represented by the upper branch of the C-shaped curve and for $X_{O_2,p}$ by the lower branch. Figures 3–6 show that for a given amount of CF_3Br in the air-stream there exists a critical value of χ_p^{-1} below which no solutions exist for the system of equations governing the structure of the inhibited flame. This critical value of χ_p represents extinction and is denoted here as χ_q. Figures 3–6 show the value of χ_q to decrease with increasing amounts of CF_3Br in the air-stream. Since the value of χ_q is proportional to the strain rate a [23], these results imply that the value of the strain rate at extinction which is denoted here by a_q, decreases with increasing amounts of CF_3Br in the air-stream. The values of T_p, T^0, $X_{O_2,p}$, $(\xi_p - \xi_{st})/\xi_{st}$ and χ_q at extinction are shown in Table 3. Also in Table 3 the values of ϵ, ν, and δ are shown.

Figure 3 shows that on the stable branch of

TABLE 2

Values of $Y_{I,2}$, $Y_{O_2,2}$, ξ_{st}, T_{st}, c_p, and q used in the Asymptotic Analysis

$Y_{I,2}$	$Y_{O_2,2}$	ξ_{st}	T_{st} (K)	c_p (kJ/(kg · K))	q
0	0.2330	0.055046	2327	1.36346	0.32707
0.05	0.2215	0.052461	2301	1.33418	0.32262
0.095	0.2108	0.050061	2294	1.29534	0.31821
0.138	0.2009	0.047829	2279	1.26497	0.31382

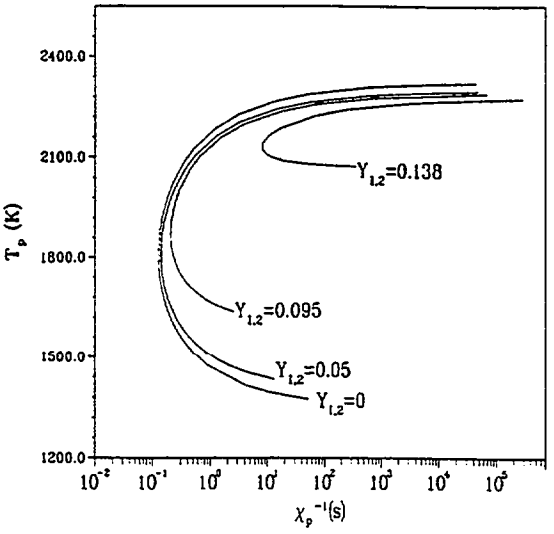

Fig. 3. The dependence of T_p on χ_p^{-1} calculated for 0%, 1%, 2%, and 3% CF_3Br by volume in the air-stream or for $Y_{I,2}$ = 0, 0.05, 0.095, and 0.138. Along each curve the amount of CF_3Br is constant.

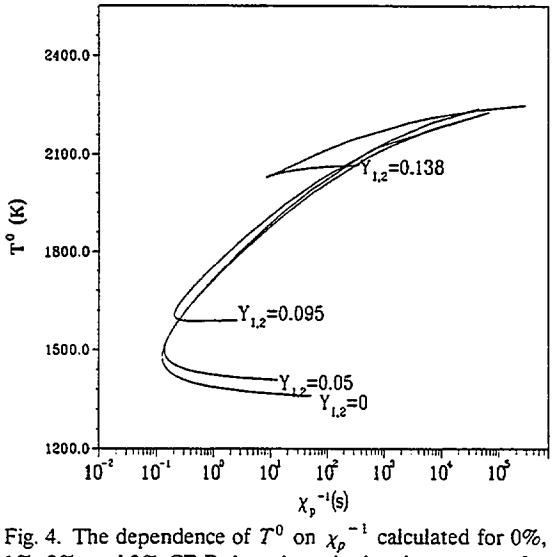

Fig. 4. The dependence of T^0 on χ_p^{-1} calculated for 0%, 1%, 2%, and 3% CF_3Br by volume in the air-stream or for $Y_{I,2}$ = 0, 0.05, 0.095, and 0.138. Along each curve the amount of CF_3Br is constant.

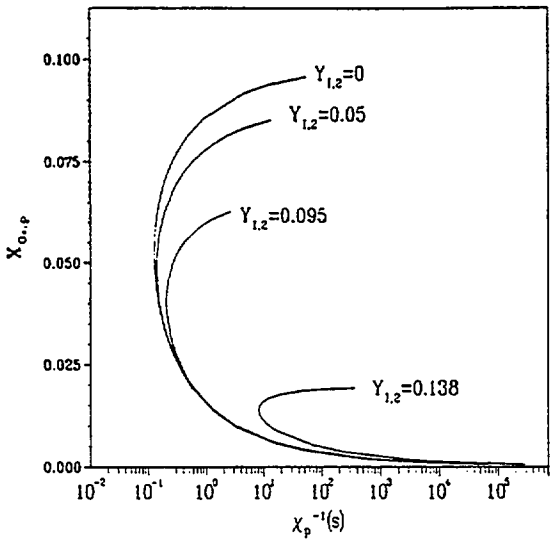

Fig. 5. The dependence of $X_{O_2,p}$ on χ_p^{-1} calculated for 0%, 1%, 2%, and 3% CF_3Br by volume in the air-stream or for $Y_{1,2}$ = 0, 0.05, 0.095, and 0.138. Along each curve the amount of CF_3Br is constant.

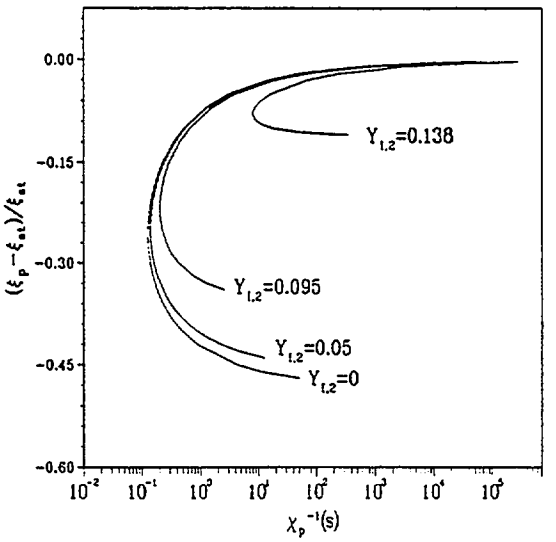

Fig. 6. The dependence of $(\xi_p - \xi_{st})/\xi_{st}$ on χ_p^{-1} calculated for 0%, 1%, 2%, and 3% CF_3Br by volume in the air-stream or for $Y_{1,2}$ = 0, 0.05, 0.095, and 0.138. Along each curve the amount of CF_3Br is constant.

the C-shaped curve the value of T_p asymptotically approaches T_{st} as $\chi_p \to 0$. Also on the stable branch of the C-shaped curve the value of T_p decreases with decreasing values of χ_p^{-1}. From Fig. 3 and Table 3 it can be observed that with increasing amounts of CF_3Br in the oxidizer stream the value of T_p at extinction increases and the difference between the values of T_{st} and T_p decreases. Figure 4 shows that the dependence of T^0 on χ_p and $Y_{1,2}$ is qualitatively similar to the dependence of T_p on these quantities. With increasing amounts of CF_3Br in the oxidizer stream, Fig. 4 and Table 3 show that at extinction the value of T^0 increases and the difference between the values of T_p and T^0 decreases. The increase in the value of T^0 at extinction with increasing amounts of CF_3Br in the air-stream is consistent with the results of previous numerical calculations [15] and measurements of temperature in the vicinity of extinction of inhibited heptane–air flames [16]. These observations clearly illustrate the inhibiting effect of CF_3Br and is attributed to the rates of production in and removal of radicals from the flame. The rates of production of radicals in the flame increases with increasing values of the flame temperature and the rates of removal of the radicals from the flame increases with increasing amounts of CF_3Br. Therefore with increasing amounts of CF_3Br the value of the temperature at which balance between the rates of production and removal of radicals from the flame is achieved also increases. Hence the value of the flame temperature in the vicinity of extinction can be expected to increase with increasing amounts of CF_3Br in the oxidizing stream.

TABLE 3

Values of Various Parameters at Extinction for Different Amounts of CF_3Br in the Air-Stream

$Y_{1,2}$	T_p (K)	T^0 (K)	$X_{O_2,p} \cdot 10^2$	$\frac{\xi_p - \xi_{st}}{\xi_{st}}$	$\chi_q(s^{-1})$	$\epsilon \cdot 10^3$	$\nu \cdot 10^3$	$\delta \cdot 10^3$
0	1759	1464	5.7087	−0.28	7.7756	10.776	7.2744	5.8132
0.05	1769	1486	5.2320	−0.27	7.0650	10.840	6.7735	5.3158
0.095	1830	1598	4.4268	−0.24	4.7529	11.649	4.7114	4.3833
0.138	2127	2029	1.4065	−0.08	0.12379	9.597	0.4789	1.1612

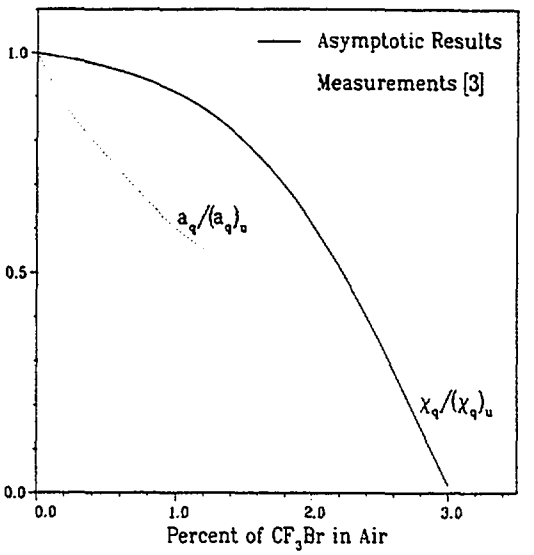

Fig. 7. Comparison between measured [3] and calculated values of the critical conditions of flame extinction for various amounts (volume percent in air) of CF_3Br added to the air-stream. The dotted lines represent the measurements and the solid line represents the asymptotic results.

Figure 5 shows that on the stable branch of the C-shaped curve the value of $X_{O_2,p}$ increases with decreasing values of χ_p^{-1}. Also in the vicinity of extinction the oxygen leakage increases rapidly with increasing values of χ_p. Figure 5 and Table 3 shows the value of $X_{O_2,p}$ at extinction to decrease with increasing amounts of CF_3Br in the air-stream. From Eqs. 9 and 11 it can be observed that the oxygen leakage through the reaction zone is proportional to the difference between the values of T_{st} and T_p. The decrease in the value of $T_{st} - T_p$ at extinction with increasing amounts of CF_3Br in the air-stream is responsible for the corresponding decrease in the value of $X_{O_2,p}$. Figure 6 shows that on the stable branch of the C-shaped curve the position of the fuel-consumption layer of the flame moves towards the oxidizer stream with decreasing values of χ_p^{-1}. Also Fig. 6 and Table 3 show the absolute value of $(\xi_p - \xi_{st})/\xi_{st}$ to decrease with increasing amounts of CF_3Br in the oxidizing stream.

Figure 7 shows comparison between the measured [3] and calculated values of the critical conditions of flame extinction for various amounts of CF_3Br added to the air-stream. The dotted line in Fig. 7 represents the measurements and the solid line represents the results of the asymptotic analysis. For counterflow methane–air diffusion flames Milne et al. [3] had measured the velocity of air (in arbitrary units) at extinction for various amounts of CF_3Br in the air-stream. In Fig. 7 the ratio of the velocity of air at extinction for the inhibited flame to that for the uninhibited flame is plotted as a function of the volume percent of CF_3Br in air, where the subscript u refers to the uninhibited flame. It has been shown previously [24, 25] that the velocity of air is proportional to the strain rate in the inviscid oxidizer flow, therefore the measured results shown in Fig. 7 roughly represent the ratio of the strain rate at extinction for the inhibited flame to that for the uninhibited flame. The asymptotic results shown in Fig. 7 represent the ratio of the value of χ_q for the inhibited flame to that for the uninhibited flame. The measurements and the calculations show the value of the strain rate at extinction to decrease with increasing amounts of CF_3Br in the air-stream. In comparison to the measurements, the asymptotic results show a weaker inhibiting effect and the differences are probably due to the approximations introduced in the asymptotic analysis, in particular the neglect of inhibition chemistry in the oxidation layer. Westbrook [5] has shown that the recombination of H radicals following from their reaction with HBr and catalyzed by Br atoms plays a significant role in inhibiting the flame. Therefore the HBr formed in the overall step V is likely to enhance the rates of recombination of H radicals in the oxidation layer thus providing stronger inhibition than that predicted by the present model.

SUMMARY AND CONCLUSIONS

An asymptotic analysis is performed to determine the influence of CF_3Br on the critical conditions of extinction of nonpremixed methane–air flames. The analysis considered addition of the inhibitor to the oxidizer stream of the nonpremixed flame. A reduced four-step mechanism consisting of the overall reactions I, II, III, and V is derived to describe the flame structure. Chemical reactions are presumed to occur in three distinct layers which are identi-

fied here as the fuel-consumption layer of thickness of order δ, the oxidation layer of thickness of order ϵ and the CF_3Br-consumption layer. The asymptotic analysis is performed for $\delta \ll \epsilon \ll 1$. The presumed structure is consistent with the results of previous numerical calculations of the structure of nonpremixed heptane–air flames [15]. In the analysis of the inner structure of the flame, the concentration of CH_4 is considered to be of order δ, the concentration of H_2 and CO of order ϵ and the concentration of the remaining species in the four-step mechanism of order unity. The fuel and the inhibitor are presumed to be consumed in different regions of the flame. The CF_3Br-consumption layer is found to be a sink for radicals and it decreases the concentration of radicals in the oxidation layer. This is the reason for flame inhibition.

The results of the asymptotic analysis are used to calculate the critical conditions of extinction of the flame with various amounts of CF_3Br added to the oxidizer stream and they are compared with previous measurements [3]. The inhibiting effect of CF_3Br predicted by the asymptotic model is found to be weaker than that measured [3]. However the predicted increase in the value of the maximum flame temperature at extinction with increasing amounts of CF_3Br in the air-stream is qualitatively in agreement with the results of previous numerical calculations [15] and measurements [16].

Future research must focus on improving the predictions of the asymptotic model. In particular Westbrook [5] has emphasized the importance of the elementary step $H + HBr \rightleftharpoons H_2 + Br$ in chemical inhibition of premixed flames by CF_3Br. Therefore this reaction must be included in future asymptotic analysis of chemical inhibition of diffusion flames. The influence of this elementary reaction on the flame structure can be illustrated by introducing steady-state approximations for Br and Br_2 and eliminating respectively the reaction rates of the elementary steps $Br + Br + M \rightarrow Br_2 + M$ and $H + Br_2 \rightleftharpoons HBr + Br$ from the balance equation for the remaining species in the five-step mechanism I′, II′, III′, IV′, and V′. This procedure will give the overall step III′. If steady-state approximation is also introduced for the H-radicals then the net rate of the overall step III is now the sum of the rates of the elementary steps 5 and $H + HBr \rightleftharpoons H_2 + Br$ [17]. If this revised rate for the overall III is included in the asymptotic analysis of the oxidation layer, with the concentration of HBr treated as a constant then the predicted inhibiting effect of CF_3Br is found to be significantly stronger than the measurements [3]. A promising approach for improving the predictions of the asymptotic model would be to merge the CF_3Br-consumption layer with the oxidation layer and include the rate of the elementary step $H + HBr \rightleftharpoons H_2 + Br$ in the asymptotic analysis of this merged layer. The resulting asymptotic analysis would be considerably more complicated than that shown here. Research along these lines is currently in progress.

The authors especially wish to thank Professor N. Peters, Professor F. A. Williams, Professor A. S. Gordon and Dr. C. K. Westbrook for many helpful suggestions and discussions. The asymptotic form of the outer structure was suggested by Professor N. Peters. This work was supported by the National Institute of Standards and Technology Grant Number NIST 60NANB3D1435 and by the National Science Foundation Grant Number NSF NIT 91-14461.

REFERENCES

1. Pitts, W. M., Nyden, M. R., Gann, R. G., Mallard, W. G., and Tsang, W., "Current Understanding," in Construction of an Exploratory List of Chemicals to Initiate the Search for Halon Alternatives, Section I, *NIST Technical Note 1279*, National Institute of Standards and Technology, U.S. Department of Commerce, pp. 14–40, August 1990.
2. Kubin, R. F., Knipe, R. H., and Gordon, A. S., in Halogenated Fire Suppresants (R. G. Gann, Ed.), *ACS Symposium Series* 16, American Chemical Society, Washington, D.C., pp. 183–207, 1975.
3. Milne, T. A., Green, C. L., and Benson, D. K., *Combust. Flame* 15:255–264 (1970).
4. Niioka, T., Mitani, T., and Takahashi, M., *Combust. Flame* 50:89–97 (1983).
5. Westbrook, C. K., *Combust. Sci. Tech.* 36:201–225 (1983).
6. Masri, A. R., *Combust. Sci. Tech.* 96:189–212 (1994).
7. Peters, N., and Rogg, B., (Eds.), *Lecture Notes in Phys.* 15 (1993).

8. Chelliah, H. K., Seshadri, K., and Law, C. K., *Lecture Notes in Phys.* 15:224–240 (1993).
9. Seshadri, K., and Peters, N., *Combust. Flame* 73:23–44 (1988).
10. Seshadri, K., and Ilincic, N., *Combust. Flame*, in press.
11. Seshadri, K., and Williams, F. A., in *Turbulent Reactive Flows* (P. A. Libby and F. A. Williams, Eds.), Academic, 1994, pp. 153–210.
12. Yang, B., and Seshadri, K., *Combust. Sci. Tech.* 88:115–132 (1992).
13. Smooke, M. D., Puri, I. K., and Seshadri, K., *Twenty-First Symposium (International) on Combustion*, The Combustion Institute, Pittsburgh, 1986, pp. 1783–1792.
14. Puri, I. K., Seshadri, K., Smooke, M. D., and Keyes, D. E., *Combust. Sci. Tech.* 56:1–22 (1987).
15. Hamins, A., Trees, D., Seshadri, K., and Chelliah, H. K., *Combust. Flame* 99:221–230 (1994).
16. Seshadri, K., and Williams, F. A., in *Halogenated Fire Suppressants* (R. G. Gann, Ed.), *ACS Symposium Series* 16, American Chemical Society, Washington, D.C., pp. 149–180, 1975.
17. Peters, N., *Lecture Notes in Phys.* 384:48–65 (1991).
18. Williams, F. A., *Combustion Theory*, Addison-Wesley Publishing Company, Redwood City, California, 1985.
19. Peters, N., *Twentieth Symposium (International) on Combustion*, The Combustion Institute, Pittsburgh, 1984, pp. 353–360.
20. Hamins, A., Thridandam, H., and Seshadri, K., *Chem. Eng. Sci.* 40:2027–2038 (1985).
21. Liñán, A., *Acta Astronaut.* 1:1007–1039 (1974).
22. Peters, N., *Combust. Sci. Tech.* 30:1–17 (1983).
23. Peters, N., *Prog. Ener. Combust. Sci.* 10:319–339 (1984).
24. Seshadri, K., and Williams, F. A., *Int. J. Heat Mass Transf.* 21:251–253 (1978).
25. Tsuji, H., and Yamaoka, I., *Twelfth Symposium (International) on Combustion*, The Combustion Institute, Pittsburgh, 1969, pp. 997–1005.

Received 21 April 1994; revised 19 August 1994

CHAPTER 3

Experimental and Numerical Studies on Chemical Inhibition of Methane-Air Diffusion Flames by CF_3Br and CF_3H

D. Trees, A. Grudno, N. Ilincic, T. Weißweiler, and K. Seshadri

Center for Energy and Combustion Research
Department of Applied Mechanics and Engineering Sciences
University of California San Diego, La Jolla, CA 92093-0411

Abstract

An experimental and numerical study was performed to characterize the influence of the addition of the fire suppressants CF_3Br and CF_3H on the structure and critical conditions of extinction of diffusion flames stabilized in the mixing layer formed between counterflowing streams of methane and air diluted with nitrogen. The critical value the strain rate at extinction was measured as function of mole fraction of CF_3Br and CF_3H added to the reactant streams. The inhibitor was added to either the oxidizer stream or the fuel stream, and the results showed that the amount of CF_3Br needed to extinguish the flame was significantly lower when mixed with the oxidizer. The experimental results were compared with numerical calculations using a detailed chemical mechanism. The calculated values of the critical conditions at extinction were found to agree well with the measurements.

Introduction

Production of the commonly used fire suppressant bromotrifluoromethane (CF_3Br) has been restricted due to its high ozone depletion potential. Nevertheless it is useful to study the mechanism of flame inhibition by CF_3Br in order to find a suitable replacement for this compound for firefighting. Literature on the use of CF_3Br in extinguishing fires and on chemical inhibition of flames has been reviewed by Ford [1] and Pitts et al. [2]. The counterflowing configuration has been used previously for studying the effects of CF_3Br on diffusion flames [3, 4, 5]. A detailed chemical-kinetic mechanism has been developed by Westbrook [6] to describe the structure of CF_3Br inhibited premixed flames burning hydrogen, methane, methanol and ethylene.

The present study focuses on elucidating the flame structure of laminar methane-air counterflow diffusion flames inhibited by CF_3Br. Extinction experiments where the agent is added to the oxidizer stream are compared with experiments with addition to the the fuel stream. Also, experiments are performed with the reactant streams diluted with nitrogen. Similar measurements are carried out with CF_3H as inhibitor. Numerical calculations using detailed chemistry [6] are performed to help understanding in detail the chemical influence of CF_3Br on the flame structure.

Experimental Apparatus and Procedure

The Burner

The counterflow burner used here is described in detail elsewhere [7]. It consists of two opposing ducts with 22.2 mm inner diameter through which the gaseous reactants are introduced. The distance between the ducts is 10 mm. A number of fine wire screens (150 mesh/inch) are placed in the ducts to ensure laminar flow at the exit of the ducts. A steady, disk shaped flame can be indefinitely stabilized in this apparatus. The combustion products are removed through a heat exchanger surrounding the lower duct into the exhaust system. A flow of nitrogen, streaming annularly around the upper duct shielded the flame from the influence of ambient air and helped preventing afterburning in the exhaust system. All measurements are made at a pressure p = 1 atm., and with the initial temperature of the reactants equal to 293 K.

The flowrates of CH_4, air, nitrogen and the gaseous agent are measured by use of calibrated variable area flowmeters and pressure gauges monitoring the inlet pressure at the flowmeters, which is kept at 10 psig. The accuracy of the measurements is estimated to be around $\pm$ 3%.

To perform an experiment, a diffusion flame is initially stabilized in the burner at predetermined values of the flowrates and the concentration of the reactants in the counterflowing streams. To ensure that the flame position which is typically close to that of the stagnation plane, is approximately in the middle of the two ducts, experiments are performed such that the rates of momentum of the counterflowing streams at the exit of the duct, represented

by the product of the density and the square of the flow velocity, are nearly the same. The agent is then added and the amount gradually increased, taking care that after each increase of the flowrate of inhibitor, the flame reached again a stable condition. When the critical amount of agent is added, the flame extinguished abruptly. The readings of the flowmeter are then recorded and the flow momentum balance recalculated, now taking the agent flow in consideration. The data are accepted only if the ratio of the two momentums is close to unity. The measurements are repeated for the same percentage of CH_4 in the fuel stream but at different values of the flowrates of the reactants. The entire set of experiments is then repeated for another dilution ratio of the reactant streams, keeping the value

$$Z_{st} = \left(1 + \frac{\nu_{O_2} M_{O_2} Y_{CH_4,fu}}{\nu_{CH_4} M_{CH_4} Y_{O_2,ox}}\right)^{-1} \tag{1}$$

constant. Here ν_i represents the stoichiometric coefficient, M_i the molecular mass, Y_i the mass fraction of a species and the subscripts ox and fu refer to oxidizer and fuel stream, respectively. If the Lewis number of all species is approximately equal to unity, then Z_{st} is the stoichiometric mixture fraction [8]. It is noteworthy that even in the presence of the inhibitor CF_3Br Eq. 1 can still be used to calculate Z_{st} [9].

The characteristic strain rate at extinction a_q is then calculated from the expression [10]

$$a_q = \frac{2|v_{ox}|}{L}\left(1 + \frac{|v_{fu}|\sqrt{\rho_{fu}}}{|v_{ox}|\sqrt{\rho_{ox}}}\right) \tag{2}$$

where L denotes the separation distance between the ducts, v the velocity and ρ the density of the reactant streams at the exit of the duct.

Numerical Calculations

A recently developed computer code [11] is used to solve the governing conservation equations under boundary conditions consistent to those in the measurements. Chelliah et al. [12] have shown that at the exit of the ducts the radial component of the flow velocity although small is not equal to zero. Since the numerical computations are performed by setting the value of the radial component of the flow velocity to zero, small misalignments between the calculated and measured profiles of the scalar quantities are to be expected.

Results and Discussions

Performing the experiments, when adding CF_3Br to the oxidizer, a second, greenish flame appearing on the oxidizer side of the CH_4-air flame can be observed. The two flames are very well distinguishable at high CF_3Br concentrations in the oxidizer stream and low reactant velocities, apparently merging at higher reactant velocities. The effect can be attributed to the reaction of CF_3Br in a "CF_3Br-consumption zone" similar to that described by Hamins

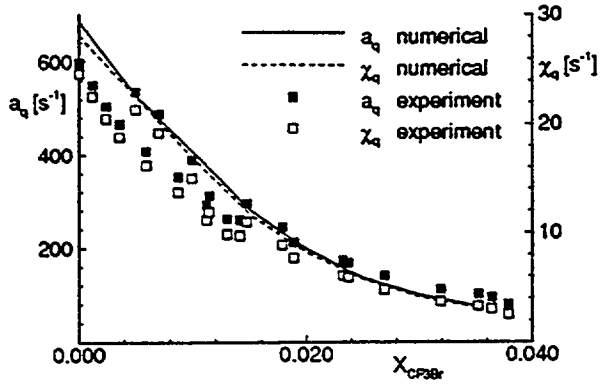

Figure 1 Experimental (points) and numerical (lines) values of the strain rate a_q and scalar dissipation rate χ_q at extinction as function of the mole fraction of CF_3Br in the oxidizer. The reactants methane and air are not diluted.

et al. [5]. The addition of CF_3Br to the fuel stream does not result in a second flame, as well as the addition of CF_3H.

Figure 1 shows experimental measurements (points) and numerical data (lines) for the strain rate a_q and the scalar dissipation rate χ_q at extinction as a function of of the mole fraction of CF_3Br in the oxidizer stream for undiluted reactants. The value of the strain rate is calculated using Eq. 2. χ_q is evaluated by [13]

$$\chi_q = \frac{a_q}{2} \frac{3\left(\sqrt{\rho_{ox}/\rho_{fl}}+1\right)^2}{2\pi\left(2\sqrt{\rho_{ox}/\rho_{fl}}+1\right)} \cdot exp\left\{2\left[\mathrm{erfc}^{-1}(2Z_{st})\right]^2\right\}^{-1} , \quad (3)$$

with a_q as defined in Eq. 2, ρ_{fl} representing the density at the locus of the highest temperature, ρ_{ox} the density in the oxidizer stream and erfc^{-1} the inverse complementary error function. To estimate ρ_{fl} for the experimental data, the density is assumed to be equal to the density of the gas mixture at the adiabatic flame temperature. The region below the curves represent flammable mixtures. The results in Figure 1 show that for increasing concentration of inhibitor in the oxidizer stream, the value of the strain rate at extinction a_q decreases. a_q can be interpreted as the inverse of a characteristic flow time, τ_f. If the gas-phase chemical reaction is approximated as a one-step process, activation energy asymptotic theories [14, 15] can predict the value of the Damköhler number at extinction δ_e, which is defined as the ratio of τ_f to a characteristic chemical time τ_c. The value of τ_c depends on the relative concentrations of the reactants and the local gas temperature. For a constant δ_e, a decrease in the value of τ_f (increase of a_q) at extinction leads to a decrease of τ_c and therefore a faster chemical reaction. Thus, the concentration of inhibitor has to decrease.

Figure 2 shows results similar to those in Fig. 1 but for CF_3Br addition on the fuel side. The mole fraction of inhibitor needed to extinguish the flame is, roughly by a factor of ten, higher than in the case of addition to the oxidizer. The numerical results, although not

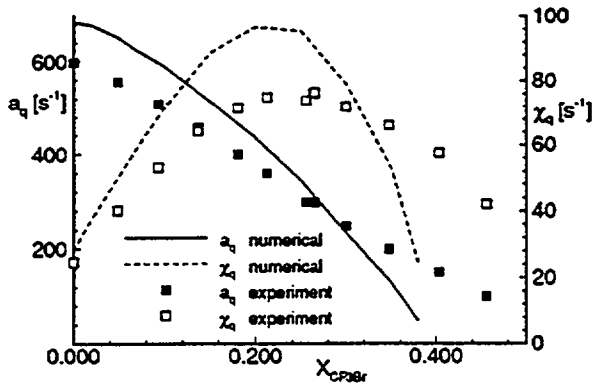

Figure 2 Experimental (points) and numerical (lines) values of the strain rate a_q and scalar dissipation rate χ_q at extinction as function of the mole fraction of CF_3Br in the fuel. The reactants methane and air are not diluted.

exactly predicting the critical conditions at extinction observed in the experiments, show a similar behavior.

The flux of CF_3Br reaching the reaction zone can be used to compare the effectiveness of CF_3Br in extinguishing the flame when it is added to the oxidizer with its effectivness when it is added to the fuel. The stoichiometry of the methane-air diffusion flame is such that the flame is located on the oxidizer side of the stagnation plane and the fuel diffuses across the stagnation plane into the reaction zone. Assuming the chemical reaction $CH_4 + 2O_2 + \nu_{CF_3Br}CF_3Br \rightarrow products$, the quantity ν_{CF_3Br} can be used as a measure of the flux of CF_3Br and calculated by $\nu_{CF_3Br} = 2X_{CF_3Br}/X_{O_2}$ in case of addition of CF_3Br to the oxidizer side, and $\nu_{CF_3Br} = X_{CF_3Br}/X_{CH_4}$ in case of addition to the fuel side. The mole fractions X_i refer to the initial conditions in the reactant streams. Figure 3 replots the experimental data

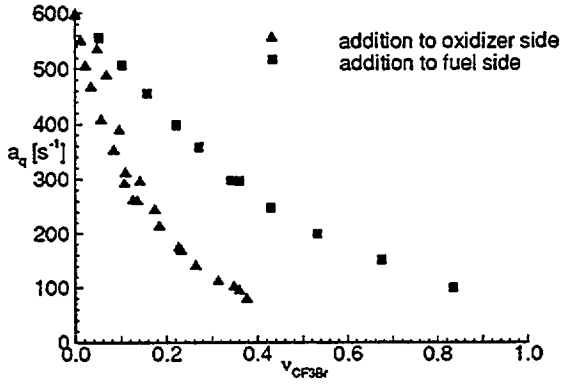

Figure 3 Comparison of the strain rate at extinction a_q for addition of CF_3Br to oxidizer and fuel as function of the calculated relative CF_3Br-concentration at the flame location.

shown in Figs. 1 and 2 in terms of this quantity ν_{CF_3Br}. It is visible that CF_3Br is, roughly by a factor of two, more efficient in quenching the flame when added to the oxidizer.

In Figures 4 and 5, experimental data for pure and diluted reactant streams are plotted.

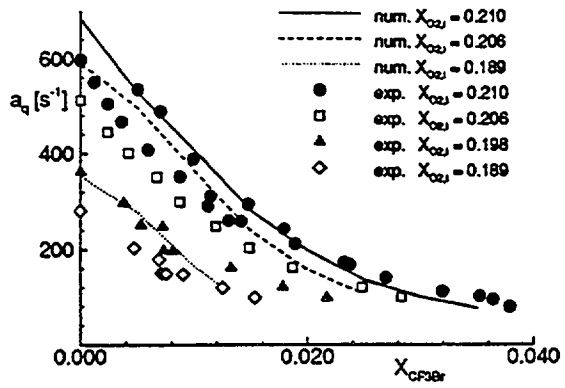

Figure 4 Experimental (points) and numerical (lines) values of the strain rate a_q at extinction as function of the mole fraction of CF_3Br in the oxidizer stream.

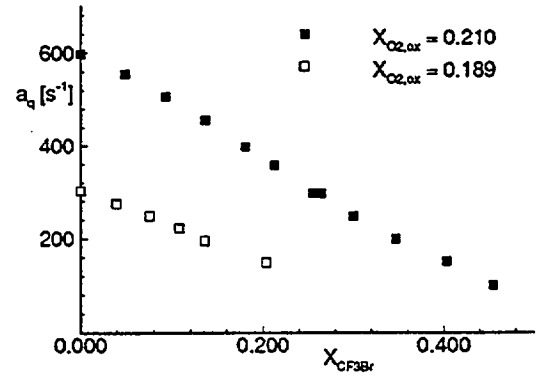

Figure 5 Experimental values of the strain rate a_q at extinction as function of the mole fraction of CF_3Br in the fuel stream.

For the case $X_{CF_3Br} = 0$, the value of the stoichiometric mixture fraction Z_{st} is kept constant for all experiments at a value of 0.0554. The parameter $X_{O_2,i}$ denotes the initial mole fraction of O_2 in the oxidizer stream, without addition of CF_3Br. The curves for the diluted cases show a behavior similar to that in the undiluted case, only the amount of CF_3Br needed to quench the flame is reduced. The numerical results for the strain rate at extinction in Fig. 4 agree well with the experimental data. This shows that the chemical-kinetic mechanism used in the calculations is capable of describing the processes in the CF_3Br inhibited flame.

In Figure 6, experimental extinction results for flames inhibited with CF_3H are shown. Comparison of Fig. 6 with Figs. 1 and 2 shows that the mole fraction of CF_3Br needed to extinguish the flame is much higher than that of CF_3Br. This result confirms that the inhibition effect of CF_3Br is mainly due to the chemical reaction of the Br atom.

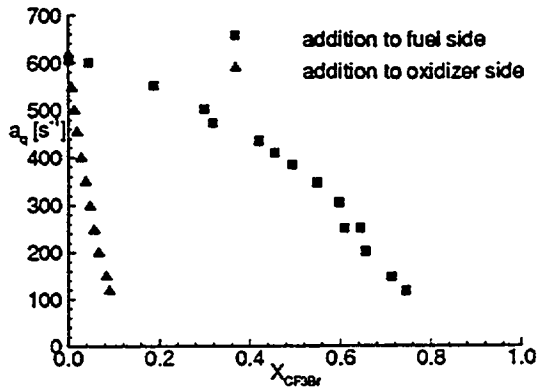

Figure 6 Strain rate at extinction a_q for addition of CF_3H to oxidizer and fuel as function of the mole fraction of the agent in the reactant stream.

Summary and Conclusions

An experimental and numerical study is performed to characterize the critical conditions of extinction and the structure of counterflow methane-air diffusion flames inhibited with CF_3Br and CF_3H. The critical conditions of extinction of the flame are measured over a wide parametric range. It is found that the chemical-kinetic mechanism employed is capable of predicting the critical conditions of extinction of methane-air flames inhibited with CF_3Br, especially if the agent is added to the oxidizer side. The experimental and numerical data show that the inhibition effect of CF_3Br is much stronger when added to the oxidizer stream of the counterflow diffusion flame. A comparison of the inhibiting effects of CF_3Br and CF_3H verifies the supposition that the Br atom plays an important role in the mechanism of flame inhibition.

References

1. Ford, C., in *Halogenated Fire Suppressants* (R. Gann, Ed.), volume 16 of *ACS Symposium Series*, Washington, DC, (1975), American Chemical Society, , pp. 1–63.

2. Pitts, W., Nyden, M., Gann, R., Mallard, W., and Tsang, W., *Construction of an Exploratory List of Chemicals to Initiate the Search for Halon Substitutes*, number 1279, National Institute of Standards and Technology, U.S. Department of Commerce, 1990, pp. 14–40, .

3. Seshadri, K., and Williams, F. A., in *Halogenated Fire Suppresants* (R. Gann, Ed.), volume 16 of *ACS Symposium Series*, Washington, DC, (1975), American Chemical Society, , pp. 149–182.

4. Niioka, T., Mitani, T., and Takahashi, M., *Combustion and Flame*, 50:89–97 (1983).

5. Hamins, A., Trees, D., Seshadri, K., and Chelliah, H., *Combust. and Flame*, 99:221–230 (1994).

6. Westbrook, C., *Combust. Sci. and Tech.*, 32:201 (1983).

7. Puri, I. K., and Seshadri, K., *Combust. and Flame*, 65(2):137–150 (1986).

8. Peters, N., *Progress in Energy and Combustion Sci.*, 10:319–339 (1984).

9. Seshadri, K., and Ilincic, N., *Combustion and Flame* (to appear).

10. Seshadri, K., and Williams, F. A., *International Journal of Heat and Mass Transfer*, 21(2):251–253 (1978).

11. Breitbach, H., Goettgens, J., Mauss, F., Pitsch, H., and Peters, N., *Twenty-Fifth Symposium (International) on Combustion*, Pittsburgh, PA, (1994), The Combustion Institute.

12. Chelliah, H. K., Law, C. K., Ueda, T., Smooke, M. D., and Williams, F. A., *Twenty-Third Symposium (International) on Combustion*, The Combustion Institute, Pittsburgh, PA, (1991), , pp. 503–511.

13. Kim, J. S., and Williams, F. A., *Journal of SIAM on Applied Mathematics*, 53(6) (1993).

14. Liñán, A., *Acta Astronautica*, 1(7-8):1007–1039 (1974).

15. Peters, N., *Combust. Sci. and Tech.*, 1982:1–17 (1982).

NIST-114
(REV. 6-93)
ADMAN 4.09

U.S. DEPARTMENT OF COMMERCE
NATIONAL INSTITUTE OF STANDARDS AND TECHNOLOGY

MANUSCRIPT REVIEW AND APPROVAL

(ERB USE ONLY)
ERB CONTROL NUMBER | DIVISION
PUBLICATION REPORT NUMBER: NIST-GCR-95-685 | CATEGORY CODE
PUBLICATION DATE: June 1996 | NUMBER PRINTED PAGES

INSTRUCTIONS: ATTACH ORIGINAL OF THIS FORM TO ONE (1) COPY OF MANUSCRIPT AND SEND TO THE SECRETARY, APPROPRIATE EDITORIAL REVIEW BOARD

TITLE AND SUBTITLE (CITE IN FULL)

Chemical Inhibition of Methane-Air Diffusion Flame

CONTRACT OR GRANT NUMBER: Grant 60NANB3D1435

TYPE OF REPORT AND/OR PERIOD COVERED: Final Report - September 15, 1993 - September 15, 1995

AUTHOR(S) (LAST NAME, FIRST INITIAL, SECOND INITIAL)
Seshadri, K.
University of California at San Diego
La Jolla, CA 92093-0411

PERFORMING ORGANIZATION (CHECK (X) ONE BOX)
[ ] NIST/GAITHERSBURG
[ ] NIST/BOULDER
[ ] JILA/BOULDER

LABORATORY AND DIVISION NAMES (FIRST NIST AUTHOR ONLY)

SPONSORING ORGANIZATION NAME AND COMPLETE ADDRESS (STREET, CITY, STATE, ZIP)
U.S. Department of Commerce
National Institute of Standards and Technology
Gaithersburg, MD 20899

PROPOSED FOR NIST PUBLICATION

[ ] JOURNAL OF RESEARCH (NIST JRES)	[ ] MONOGRAPH (NIST MN)	[ ] LETTER CIRCULAR
[ ] J. PHYS. & CHEM. REF. DATA (JPCRD)	[ ] NATL. STD. REF. DATA SERIES (NIST NSRDS)	[ ] BUILDING SCIENCE SERIES
[ ] HANDBOOK (NIST HB)	[ ] FEDERAL INF. PROCESS. STDS. (NIST FIPS)	[ ] PRODUCT STANDARDS
[ ] SPECIAL PUBLICATION (NIST SP)	[ ] LIST OF PUBLICATIONS (NIST LP)	[X] OTHER NIST-GCR
[ ] TECHNICAL NOTE (NIST TN)	[ ] NIST INTERAGENCY/INTERNAL REPORT (NISTIR)	

PROPOSED FOR NON-NIST PUBLICATION (CITE FULLY) [ ] U.S. [ ] FOREIGN

PUBLISHING MEDIUM
[ ] PAPER [ ] CD-ROM
[ ] DISKETTE (SPECIFY)
[ ] OTHER (SPECIFY)

SUPPLEMENTARY NOTES

ABSTRACT (A 2000-CHARACTER OR LESS FACTUAL SUMMARY OF MOST SIGNIFICANT INFORMATION. IF DOCUMENT INCLUDES A SIGNIFICANT BIBLIOGRAPHY OR LITERATURE SURVEY, CITE IT HERE. SPELL OUT ACRONYMS ON FIRST REFERENCE.) (CONTINUE ON SEPARATE PAGE, IF NECESSARY.)

The principle objective of this research is to clarify the mechanisms of chemical inhibition of methane-air diffusion flames by CF_3Br and CF_3H. An experimental, numerical and analytical study is conducted. In inhibited flames at conditions close to flame extinction significant amount of oxygen is found to leak through the reaction zone. Therefore an asymptotic analysis is performed to characterize the structure and critical conditions of extinction of uninhibited methane-air diffusion flames. Later this analyses is extended to methane-air diffusion flames inhibited with CF_3Br. Critical conditions of extinction of the flame are measured over a wide range with agents added to the air stream and to the fuel stream. Numerical calculations with detailed chemistry are performed to calculate the structure and critical conditions of flame extinction. The numerical results are compared with the measurements.

KEY WORDS (MAXIMUM OF 9; 28 CHARACTERS AND SPACES EACH; SEPARATE WITH SEMICOLONS; ALPHABETIC ORDER; CAPITALIZE ONLY PROPER NAMES)
air; bromotrifluoromethane; carbon monoxide; chemical inhibition; diffusion flames; fire research; hydrogen; methane; triflormethane; water

AVAILABILITY
[X] UNLIMITED [ ] FOR OFFICIAL DISTRIBUTION - DO NOT RELEASE TO NTIS
[ ] ORDER FROM SUPERINTENDENT OF DOCUMENTS, U.S. GPO, WASHINGTON, DC 20402
[X] ORDER FROM NTIS, SPRINGFIELD, VA 22161

NOTE TO AUTHOR(S): IF YOU DO NOT WISH THIS MANUSCRIPT ANNOUNCED BEFORE PUBLICATION, PLEASE CHECK HERE. [ ]

WORDPERFECT